



VCU

Virginia Commonwealth University
VCU Scholars Compass

Theses and Dissertations

Graduate School

2009

Band Bending in GaN

Michael Foussekis

Virginia Commonwealth University

Follow this and additional works at: <https://scholarscompass.vcu.edu/etd>



Part of the [Physics Commons](#)

© The Author

Downloaded from

<https://scholarscompass.vcu.edu/etd/1781>

This Thesis is brought to you for free and open access by the Graduate School at VCU Scholars Compass. It has been accepted for inclusion in Theses and Dissertations by an authorized administrator of VCU Scholars Compass. For more information, please contact libcompass@vcu.edu.

Band Bending in GaN

A thesis submitted in partial fulfillment of the requirements for the degree of Master of Science in Physics / Applied Physics at Virginia Commonwealth University.

By

Michael A. Foussekis

B.S. in Physics

Virginia Polytechnic Institute and
State University, 2007

M.S. in Physics/Applied Physics

Virginia Commonwealth University, 2009

Directors:

Mikhail A. Reshchikov, Associate Professor, Department of Physics

Alison. A. Baski, Department Chair, Department of Physics

Virginia Commonwealth University,
Richmond, Virginia, 23284

5-08-2009

Acknowledgments

I am very thankful for all of the help and support I have received during this thesis. Without this support this work would not be possible.

I would first like to thank my family for pushing me to further my education career. Both of you have been very supportive and I thank you. My parents have taught me to work hard and I have tried to bring this attitude to my work at VCU. I would also like to thank my sister for all time spent relaxing together. This was very helpful in keeping my sanity.

This thesis would not be possible without the support and guidance of my academic advisors, Dr. Alison Baski and Dr. Mikhail Reshchikov. I would like to thank them for their patience and time spent teaching me how to become a successful researcher. Vince Ong, Joe Ferguson, Jose Ortiz, Crystal Storey, Monika Ruchala and Dr. Chris Moore were instrumental in my work on this thesis. I would also like to thank Janice Guyer and Evelyn Perham for making me feel at home, here at VCU.

I owe Dr. Marilyn Bishop a debt of gratitude for truly teaching me physics and not simply cramming problems down my throat, as fun as that sounds. Thank you for having so much patience as when I spent hours asking you questions about homework.

I would also like to thank Kate Golkow for being supportive of me during this process. I am sure that I have bored you to death countless times with my ramblings about band bending. Thank you for your love and patience; you have pushed me to succeed in whatever I do. I am grateful for all of your encouragement and love.

I again want to thank EVERYONE at the VCU Physics Department!

Table of Contents

Acknowledgments.....	ii
Table of Contents.....	iii
List of Figures.....	iv
Abstract.....	v
Chapter 1: Gallium Nitride.....	1
1.1 Motivation.....	1
1.2 Literature Review.....	2
Chapter 1 Figures.....	5
Chapter 2: Measurement Techniques.....	8
2.1 Kelvin Probe.....	8
2.2 Atomic Force Microscopy.....	10
2.3 Photoluminescence.....	12
Chapter 2 Figures:.....	14
Chapter 3: Simple Model of Band Bending in GaN.....	18
Chapter 4: Surface Potential Measurements of GaN.....	24
4.1 Spectral Response.....	24
4.2 Intensity Dependence.....	25
4.3 Effect of Environment.....	25
4.4 Photoluminescence Measurements.....	26
4.5 Decay of SPV.....	27
4.6 Effect of Temperature.....	27
Chapter 4 Figures:.....	29
Chapter 5: Conclusions.....	40
Appendix.....	41
How to use the Kelvin Probe.....	41
How to Perform SKPM on the AFM.....	45
References.....	48

List of Figures

Fig. 1.1: A unit cell for GaN which has a hexagonal wurtzite structure. Lattice constant values: $a = 3.19\text{\AA}$ and $c = 5.19\text{\AA}$.	5
Fig. 1.2: Three possible planes for GaN which include the c , m and a -planes.	6
Fig. 1.3: Schematic for band bending during illumination, where electron-hole pairs are created in the depletion region.	7
Fig. 2.1: (a) Sample and probe not in electrical contact; (b) Sample and probe brought into electrical contact; (c) $V_{\text{cpd}} = V_{\text{backing}}$ with no charge/current.	14
Fig. 2.2: Schematic showing how band bending is related to contact potential V_{cpd} .	15
Fig. 2.3: Kelvin probe setup with illumination performed from the backside.	16
Fig. 2.4: Schematic of Scanning Kelvin Probe Microscope (SKPM).	17
Fig. 4.1: Steady-state photovoltage spectrum for undoped GaN750 at 295 K in air ($P = 6 \times 10^{16} \text{ cm}^{-2} \text{ s}^{-1}$).	29
Fig. 4.2: Steady-state photovoltage spectrum for Si-doped GaN595 at 295 K in air ($P = 6 \times 10^{16} \text{ cm}^{-2} \text{ s}^{-1}$).	30
Fig. 4.3: CPD transients (RT, air) obtained with illumination at 580 nm with various intensities.	31
Fig. 4.4: Dependence of SPV saturation on light intensity at 295 K in air.	32
Fig. 4.5: Schematic of pump-purge system.	33
Fig. 4.6: SPV steady state behavior as a function of environment for GaN750.	34
Fig. 4.7: SPV steady state behavior as a function of environment for GaN595.	35
Fig. 4.8: Evolution of PL intensity for GaN750 in air under continuous exposure (HeCd laser).	36
Fig. 4.9: Decay rates shown for GaN750 after illumination with 365 nm light for different exposure times and environments.	37
Fig. 4.10: Decay rates for GaN750 under different environments at 295 K (~3 h exposures).	38
Fig. 4.11: Decay rates shown for GaN750 under vacuum at 295 and 400 K.	39

Abstract

Band Bending in GaN

By Michael A. Foussekis

A thesis submitted in partial fulfillment of the requirements of the degree of Master of Science at Virginia Commonwealth University. Virginia Commonwealth University, 2009.

Major Director: Dr. Mikhail Reshchikov, Assistant Professor, Department of Physics
Dr. Alison A. Baski, Associate Professor, Department of Physics

Steady-state and transient surface photovoltages in undoped GaN are studied in various environments (air, nitrogen, oxygen, vacuum) at room temperature and 400 K with a Kelvin probe attached to an optical cryostat. The results are explained within a phenomenological model accounting for the accumulation of photo-generated holes at the surface, capture of free electrons from the bulk over the near-surface potential barrier, and emission of electrons from surface states into the bulk. Mechanisms of surface photovoltage are discussed in detail. Photoadsorption and photodesorption of negatively charged species will either increase or decrease the surface potential and thus band bending. Oxygen is the assumed species responsible for the SPV changes in air ambient during continuous UV illumination. This variation in SPV will be confirmed with photoluminescence measurements.

Chapter 1: Gallium Nitride

1.1 Motivation

Gallium Nitride (GaN) is a wide band gap semiconductor (~ 3.43 eV at 295 K) which has many properties that make it promising for use in electronic and optical devices. The creation of the first GaN-InGaN laser diode (LD) was an important breakthrough in GaN research. Lasers sold on the commercial market usually have lifetimes of 10,000 hours. When GaN-InGaN LD's reached this lifetime, an immediate application of this technology was data storage (Blue ray/DVD). Compact discs (CDs) are typically written with a wavelength close to 780 nm, which is in the infrared region of the spectrum. Using a GaN LD in these devices write and read with a shorter wavelength (400 nm) which allows for four times the recording density.^{1,2} In the 1990s, performance of GaN devices began to improve drastically. This led to the production of commercial GaN based light emitting diodes (LEDs). These are able to give off intense light in the blue and the green regions of the spectrum at a low energy cost.^{1,2}

GaN is a very stable material which has a melting point of about 2500 °C, and a high thermal conductivity of $1300 \text{ Wm}^{-1}\text{K}^{-1}$.² GaN is an exceptionally stable compound which exhibits structural hardness.³ The inherent chemical stability of GaN at high temperatures, combined with its structural stability, makes it an appealing material for protective coatings and devices. GaN is an excellent candidate for devices which operate in high temperature environments and require a wide band gap.⁴ GaAs and Si devices do not operate well under these extreme conditions. Because of the properties mentioned previously, GaN has proven to be a promising material for devices.

Progress is being made in the understanding of bulk and surface defects in GaN. This will aid the development of higher quality GaN that can be used in light emitting and electronic devices. The weak understanding of defects is a detriment to the efficiency and reliability of devices fabricated from GaN.⁵ Despite tremendous progress in research of these defects, their role in the material and their influence on device performance are not yet

completely understood.⁶ In this thesis, band bending in GaN is investigated through the use of photoluminescence and a Kelvin probe setup.

1.2 Literature Review

Gallium Nitride (GaN) was first synthesized by W. C. Johnson in 1932.⁷ In August 1969, Maruska and Tietjen established that GaN could be grown with a high enough purity to be used in electrical and optical devices.⁸ The technique involved with the growth of these samples was hydride vapor phase epitaxy (HPVE). GaN was known to have many promising electrical and optical properties, but further research was required to find an ideal substrate material. There was no suitable material to use as a GaN substrate at the time.⁹

The growth of high quality GaN films for the creation of devices was no easy task. Challenges included large spatial defect densities and inherent chemical stability. When GaN is grown as a thin film on a variety of substrates, they tend to have a high density of spatial defects due to poor lattice match.^{8,9} The first good quality epilayers were grown by Yoshida et al. in 1983. This was achieved through the use of a new growth technique involving two steps. The process involved using an AlN buffer layer between the GaN and sapphire substrate.¹⁰ This buffer layer greatly improved the quality of the GaN crystal and helped solve the problem of the lattice mismatch. Amano et al. were the first to show that the growth of p-type conducting GaN films was possible.¹¹ This process was discovered while the group was trying to study cathode luminescence in Mg-doped GaN film. In this research, it was shown that low energy electron beam irradiation (LEEBI) caused p-type conduction in the GaN films.¹² With this breakthrough, Akasaki et al. was able to create the first p-n junction in a blue LED in 1989.¹³ Nakamura improved p-type quality by demonstrating that annealing the GaN film after growth results in a greater hole concentration and improved performance.¹⁴ Nakamura's research brought the production of GaN LEDs to a point where they could be commercially sold and manufactured.^{1,14} GaN LEDs have been mass produced

and commercially used in many of today's devices with further research needed to make improvements.

Gallium nitride naturally forms a wurtzite crystalline structure under ambient conditions.¹⁵ This structure is the combination of two hexagonal closed-packed (HCP) lattices which are intermeshed. The unit cell of GaN can be seen in Fig1.1. If the unit cell is extrapolated in three dimensions, it would form the HCP lattice. Calculations have shown that the average distance between the Ga and N atoms in bulk is 1.95 Å. Maruska et al. reported lattice constant values of $a = 3.19$ Å and $c = 5.19$ Å.¹⁶ In this study, the surfaces of c-plane GaN films grown on a sapphire substrate will be examined. This is the most commonly grown GaN plane, some others being m-plane and a-plane shown in Fig. 1.2. In this diagram the differences between each plane due to the termination of the crystal lattice are schematically shown. The c-plane is a polar plane that terminates with Ga atoms on one side and N atoms on the other. Due to higher crystal quality, c-plane GaN grown on c-plane sapphire is generally used in LED fabrication. A problem with c-plane GaN LEDs, however, is the quantum confined stark affect which decreases LED efficiency.¹⁷

GaN films grown on c-plane sapphire through various techniques are discussed in this thesis. Undoped and Si-doped GaN layers with 1 to 3 μm thicknesses were grown using molecular beam epitaxy (MBE) and metal organic vapor chemical deposition (MOVCD) by Prof. H. Morkoç's group in the Electrical Engineering Department at Virginia Commonwealth University. The concentration of free electrons in these samples ranged from 3×10^{16} to $7 \times 10^{18} \text{ cm}^{-3}$. The two samples studied in more detail were grown by MBE and are designated GaN750 (un-doped) and GaN595 (Si-doped). Doping of a GaN film with Si leads to a higher concentration of electrons and narrower depletion region.

Most surface potential studies of GaN have focused on analyzing defects and their properties.¹⁸ Threading dislocations have been found to decrease the Fermi energy and increase the work function of GaN by around 0.1 to 0.2 eV.¹⁹ Extensive measurements have been done to measure the amount of band bending in n-type GaN. Studies of GaN have

shown that the surface band bending is around 0.4 to 1.1 eV.²⁰ In particular Dahlberg et al investigated photovoltage transients in GaP and observed a logarithmic dependence of band bending with light intensity.²¹ The band bending in GaN was determined by XPD and by an AFM in Kelvin probe mode.²³ Measurements showed that band bending in dark varied from 0.7 to 1.5 eV. It was also shown that band bending increased with the concentration of free electrons.²² Research has also been done on the chemisorption of oxygen on the surface of GaN(0001) (c-plane). Bermudez et al. showed that band bending is ~0.5 eV less than on atomically clean surfaces.²³ A logarithmic variation of the photovoltage has been observed, which typically was in the range of 10^{-2} - 10^2 s. This is attributed to thermionic emission of electrons from the bulk to the surface states over the barrier near the surface.²⁴ Bermudez has shown that surface treatments can also affect the amount of surface band bending.²⁵ Effects of annealing, ion bombardment and cleaning techniques were investigated. Band bending can be reduced 0.3 to 0.5 eV through UV illumination.²² This happens due to electron-hole pair separation which will be explained in the theory section.

Chapter 1 Figures

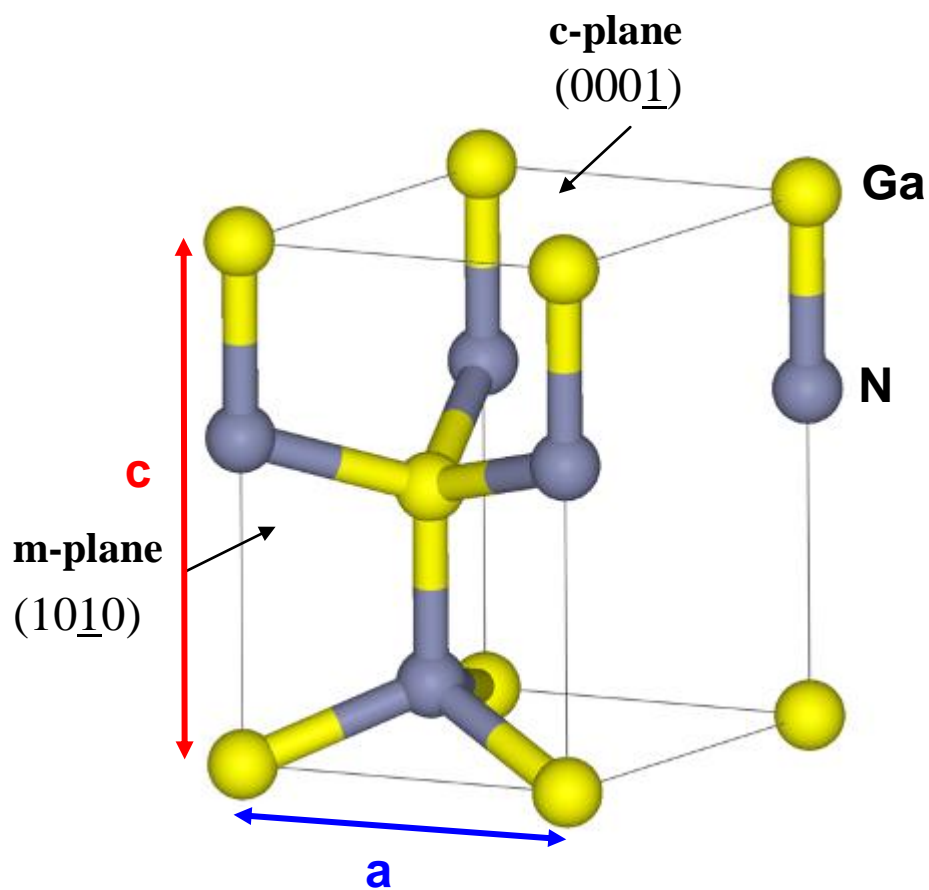


Fig. 1.1: A unit cell for GaN which has a hexagonal wurtzite structure. Lattice constant values: $a = 3.19\text{\AA}$ and $c = 5.19\text{\AA}$.

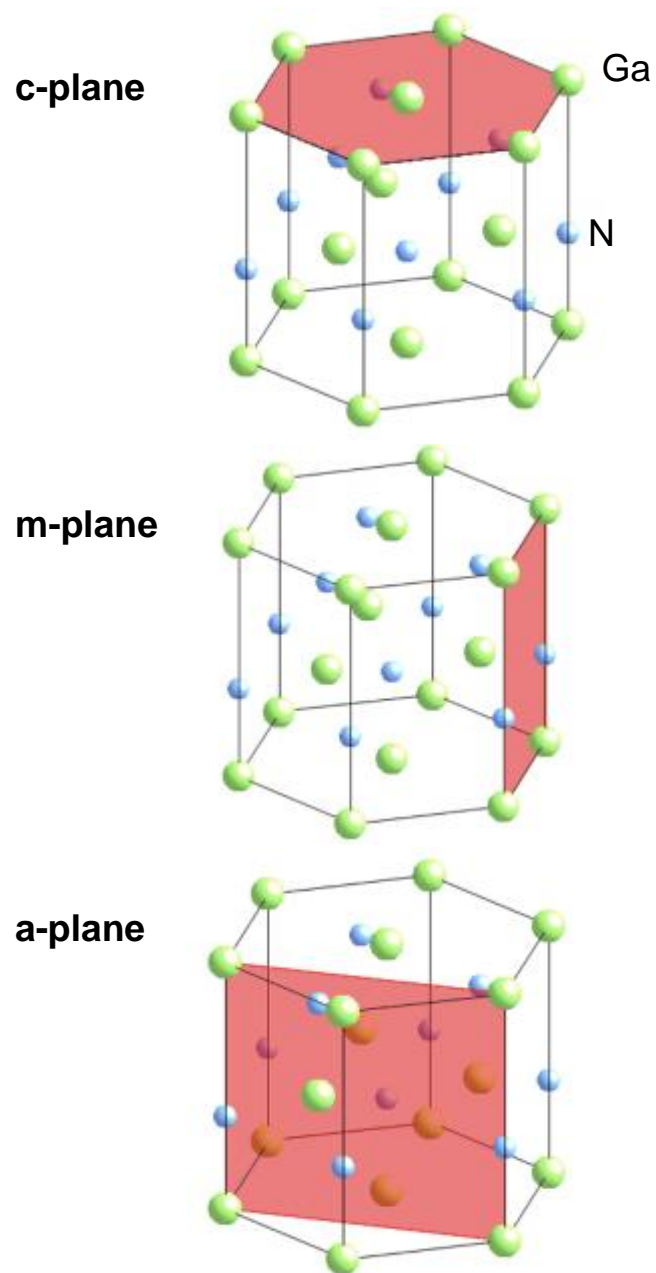


Fig. 1.2: Three possible planes for GaN which include the c , m and a -planes.

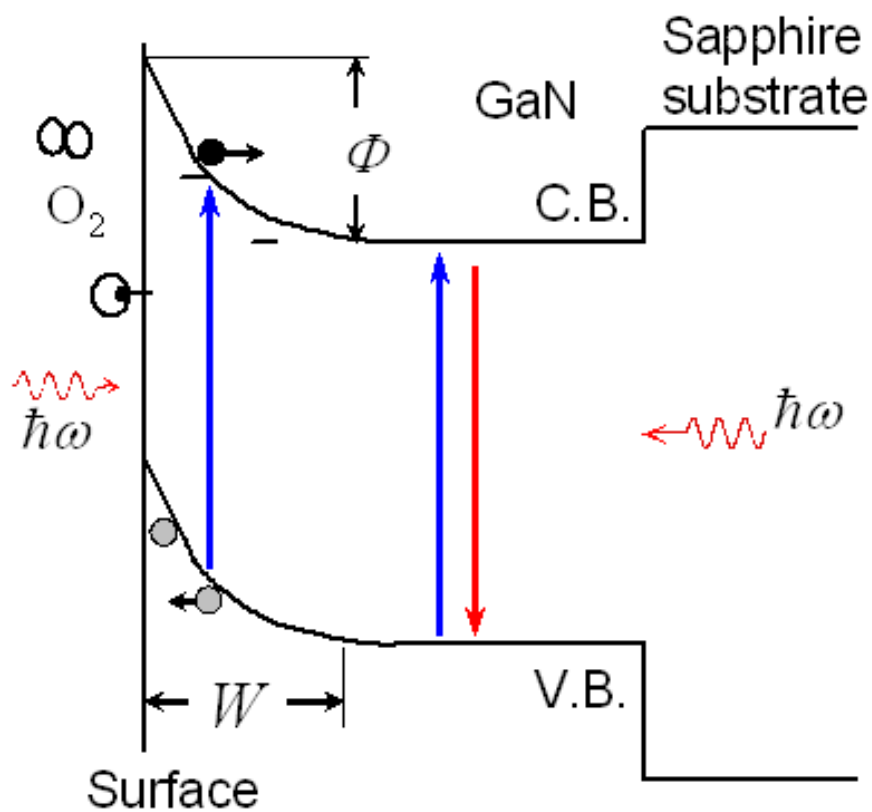


Fig. 1.3: Schematic for band bending during illumination, where electron-hole pairs are created in the depletion region.

Chapter 2: Measurement Techniques

2.1 Kelvin Probe

The Kelvin probe is a measurement device that resembles a vibrating capacitor and measures the difference in work functions between two materials. The materials measured can be liquid interfaces, metals, or semiconductors. William Thomson postulated the Kelvin probe technique around 1861, and N. Knoble was the first person to utilize a constantly vibrating reference probe in 1932. The Kelvin probe is a tool used to measure the contact potential difference (CPD) between two materials with high precision. This technique can obtain a 1 meV resolution. The method is very precise, but not accurate, in determining the absolute values of work functions. This low accuracy is due to various changes in the environment or system settings which affect the CPD's absolute value.²⁶ In our experiments the absolute value of the CPD measured many times over a period of more than six months was reproducible to within an accuracy of 0.05 eV for a single sample.

The Kelvin probe (KP) used in this work (McAllister KP6500) consists of a vibrating reference probe and a stationary sample which are arranged in a parallel plate configuration. Figure 2.1a shows the sample and probe isolated from each other. In Fig 2.1b, the sample and probe are brought into electrical contact, causing a flow of charge from the material with the higher Fermi energy to the lower one. This flow of charge leaves each “plate” of the capacitor oppositely biased. After the sample and probe are brought into electrical contact (Fig 2.1c), the Kelvin probe applies a “backing potential” to the reference probe. This potential is swept through desired voltages and nullifies the potential difference between the two plates. When no backing potential is applied, there exists a CPD between the plates due to the difference in work functions. This difference is defined as

$$eV_{cpd} = \Delta_{workfunction}$$

While the voltages are being swept, this potential difference generates a current in the circuit. The KP monitors this current and when $V_{backing} = -V_{cpd}$, the electric field between the plates

has been nullified, i.e., no current output.²⁶ In order to improve accuracy, the Kelvin probe oscillates the probe, effectively changing the capacitance C given by:

$$C = \frac{\varepsilon\varepsilon_o A}{d} = \frac{Q}{IR} \quad , \quad (1)$$

where d is the distance between the sample surface and the probe. It can be seen from Eq(1) that changing the probe-to-sample distance will also create a current if the charge Q and resistance are kept constant. The Kelvin probe measures the current during operation and records the V_{cpd} when no current is detected. Therefore, changes in the work functions can be effectively monitored.

The Kelvin probe only monitors the current to measure the CPD. The KP exploits a relationship between the current and the CPD. The measured current depends on the oscillation amplitude, the probe-to-sample distance and oscillation frequency:

$$i = \frac{dQ}{dt} = \Delta V \frac{dC}{dt} \quad , \quad (2)$$

where Q is the charge on the plates, C is the capacitance, and ΔV is the potential difference between probe and sample. It is important to note that $\Delta V = V_{backing} + V_{cpd}$ in these calculations. The distance between the probe and sample is varied sinusoidally as:

$$d = d_o + d_1 \sin(\omega t + \phi) \quad (3)$$

After substituting Eq(3) into Eq(2) and taking a time derivative of d , the current i as a function of ΔV is given by:

$$i = -\varepsilon\varepsilon_o A (\Delta V) \frac{d_1 \omega \cos(\omega t + \phi)}{[d_o + d_1 \sin(\omega t + \phi)]^2} \quad (4)$$

Eq(4) demonstrates that the current is linearly related to the contact potential difference. The Kelvin probe exploits this linear relationship by scanning the backing potential while measuring the current. To improve the signal-to-noise ratio, the KP probe uses an oscillating AC signal. The KP software uses interpolation or extrapolation to then determine the null point, which is where $V_{backing} = -V_{cpd}$. This is done instead of measuring the null point directly because the signal-to-noise ratio is improved. Therefore, low-noise data can be acquired by

exploiting this linear relationship between the CPD and current. From the measured CPD, the absolute value of band bending can be calculated using Eq(6) in Chapter 3. This is illustrated in Fig 2.2 where all the values except band bending remain relatively constant throughout the measurement period. The Kelvin probe is an excellent, non-invasive device used to measure the surface potential of materials.

The Kelvin probe used in this study was a McAllister KP6500 ultra high vacuum (UHV) instrument. A cross-section of our setup is schematically shown in Fig 2.3. Environmental conditions can be altered because the Kelvin probe is mounted inside an optical cryostat. The temperature can be varied from 200 to 400K and the environment can be changed to be air ambient, nitrogen, oxygen, or vacuum. Illumination in the current setup is done through the backside of the sample or sapphire substrate. This geometry has given a better signal-to-noise ratio than illumination from the front side. Since the bandgap of sapphire is much larger than the wavelengths of light used for illumination this orientation does not affect our measurements. Illumination in our experiments was performed with a 75 Watt xenon lamp attached to a monochromator. Light exiting the monochromator slit is filtered with an additional set of band pass filters to completely block any stray light. Control measurements have been done to measure the difference between illumination from the front side (through a port at 45° and by using a perforated probe) and backside. It has been found that there is no quantitative difference in the SPV values and their transients in these two geometries.

2.2 Atomic Force Microscopy

The Atomic Force Microscope (AFM) is a tool that allows researchers to measure surface properties through the use of a micro-machined cantilever. The AFM can be equipped with a conductive tip and a CAFM or TUNA module to also measure the electrical properties of a sample. The AFM used in this research was a Veeco Nanoscope IIIa Dimension 3100. Our

setup is also capable of a technique known as Scanning Kelvin Probe Microscopy (SKPM) which measures the surface potential.

In 1985, G. Binnig, C. Quate, and C. Gerber published a paper proposing the AFM technique. This technique can measure ultra-small forces ($\sim 10^{-9} N$) on objects as small as atoms. To measure such forces, an AFM typically monitors the deflections of a cantilever using a laser reflected from the backside of the cantilever. In the reports of Binnig et al. the cantilever consisted of a gold foil with a diamond tip attached. A laser was focused onto the backside of the cantilever and deflections of the laser beam were monitored using a photodiode. The forces acting between the tip and sample originate from Van der Waals, electrostatic, capillary, chemical forces.²⁷

In AFM operation a tip with a micro-machined cantilever is oscillated and brought into contact with the surface. These tips are generally made of silicon or silicon nitride and have both a high resonant frequency and small force constant. This is due to the relation

$$\omega = \sqrt{\frac{k}{m}},$$

where the small cantilever mass results in a sufficiently high frequency for low force constant k . The tips may also have additional coatings to improve properties such as their conductance. Reflections of a laser beam which is directed at the backside of the tip will monitor the amount of deflection, which can be converted into units of force. This is done through the use of a photodetector which converts the laser beam position to an electrical signal corresponding to an amount of deflection. This deflection signal is then sent to a feedback circuit which moves the tip vertically to maintain a constant force between the sample and tip. The tip-height data are then displayed as surface topography with the tip scanning an x-y image.

The main operation mode of the AFM used in this research is scanning Kelvin probe microscopy (SKPM). This method was introduced in 1991 as a non-contact technique to measure the surface potential using an AFM. SKPM works on the same premise as the

Kelvin probe, but on a microscopic scale. Unlike the Kelvin probe, the SKPM technique detects the local surface potential in a nanometer-range area. The technique is shown schematically in Fig 2.4. First, the AFM scans the topography and stores these data into memory. Once this is done, the tip lifts to a pre-set height above the sample (50–100 nm) and retraces the topography in order to keep a constant distance between the probe and sample. While retracing the topography, the surface potential is then measured. This is done by biasing the tip with an external voltage ($V_{DC} + V_{AC} \sin \omega t$) where ω is the resonant frequency of the cantilever. When this voltage is applied, the tip experiences a force given by

$$F = -\frac{\partial U}{\partial z} = \frac{dC}{dz} V_{DC} V_{AC},$$

where U is the electric potential energy and C is the capacitance between the tip and sample. After substitution,

$$F_{\omega} = -\frac{dC}{dz} (V_{TIP} - V_{SAMPLE}) V_{AC} \sin(\omega t)$$

$$\text{where } (V_{TIP} - V_{SAMPLE}) = V_{CPD}$$

To obtain the CPD from this force, the DC voltage is varied by the feedback loop to zero out the $\sin(\omega t)$ component of the force. When the force is zero the voltage applied is equal to the contact potential difference similar to the Kelvin probe.²⁸

In our measurements illumination of the sample in the AFM setup can be done with a UV lamp or laser. Caution needs to be taken when illuminating because stray light can affect the laser signal at the photodiode.

2.3 Photoluminescence

Photoluminescence (PL) is the spontaneous emission of light caused by photons which excite electrons into higher energy states. This creates electron-hole pairs which recombine shortly after formation in most cases. After this recombination occurs, a photon less than or equal in energy to the excitation energy is emitted. Generally, the time between excitation and

emission is on the order of nanoseconds, but in some cases can be extended to minutes. By measuring the emitted light spectrum from the sample, one can measure energy levels and allowed energy transitions. PL is a technique that has been used to measure defects in various semiconductors including GaN.²⁹

In GaN, PL excites electrons from the valence band to the conduction band. When GaN is illuminated from the surface, electron hole pairs are created in the depletion region where a strong electric field separates them. Due to this fast separation there is almost no recombination in the depletion region. This means that the depletion region width plays a significant role in the intensity of the PL signal. As previously stated, the depletion region width has a quadratic relation to band bending. It is important to remember that an increase in PL signal corresponds to a decrease in band bending.³⁰ PL measurements have been performed on our GaN samples, as well as monitoring the PL signal intensity over time.

Chapter 2 Figures:

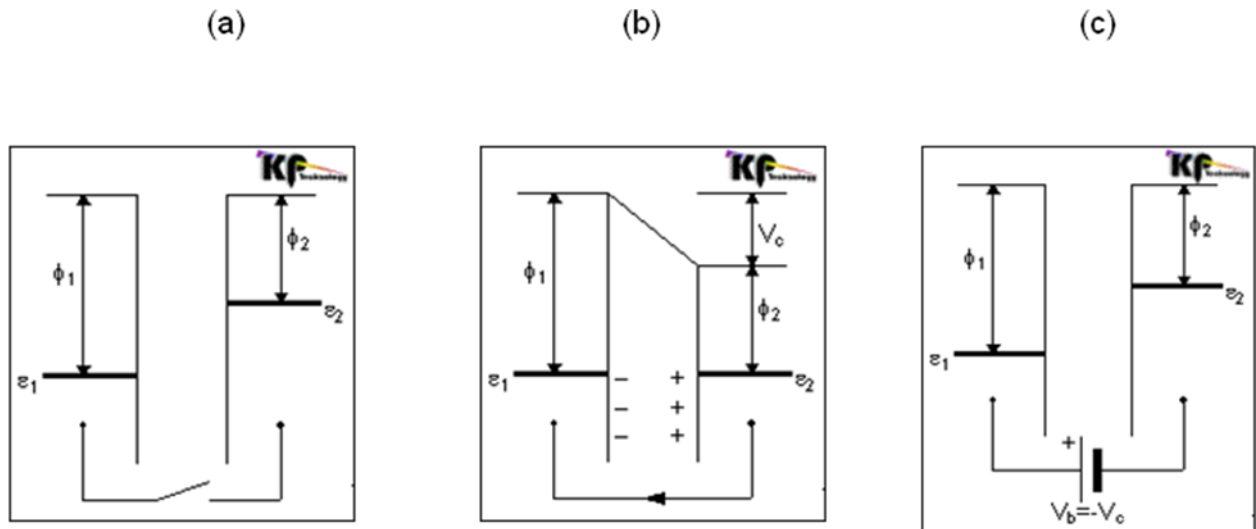


Fig. 2.1: (a) Sample and probe not in electrical contact; (b) Sample and probe brought into electrical contact; (c) $V_{cpd} = V_{backing}$ with no charge/current.

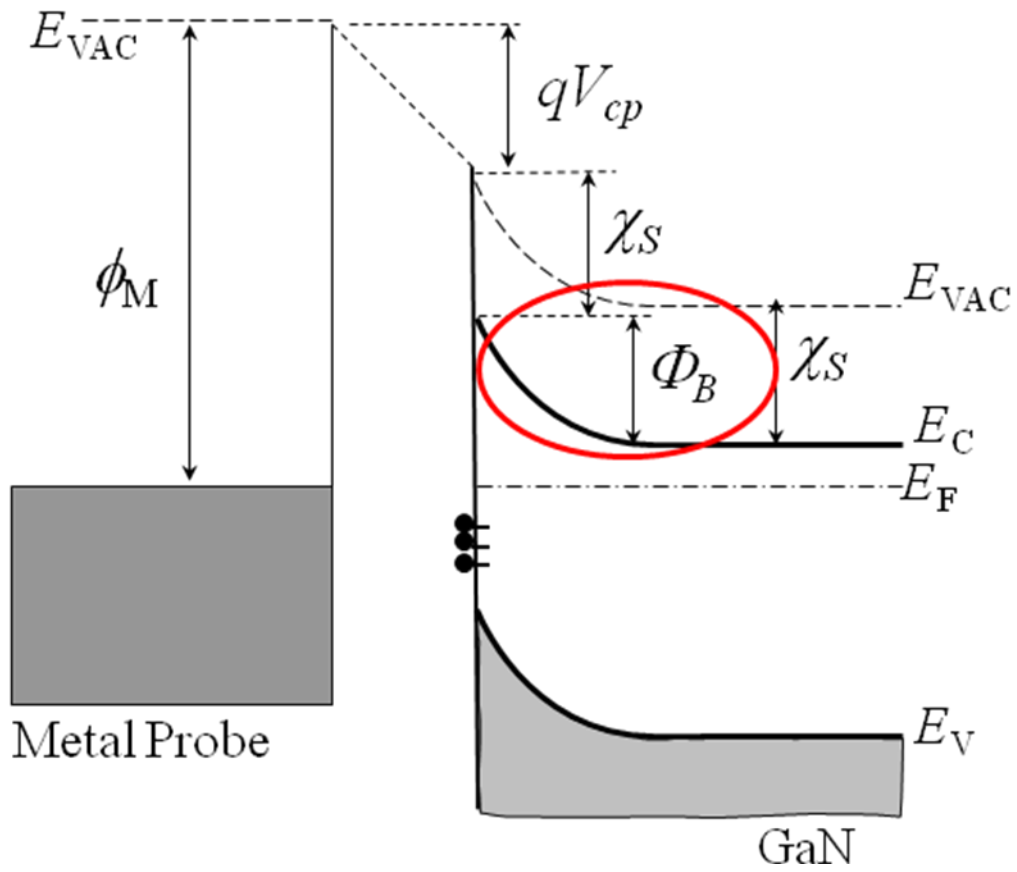


Fig. 2.2: Schematic showing how band bending is related to contact potential V_{cpd} .

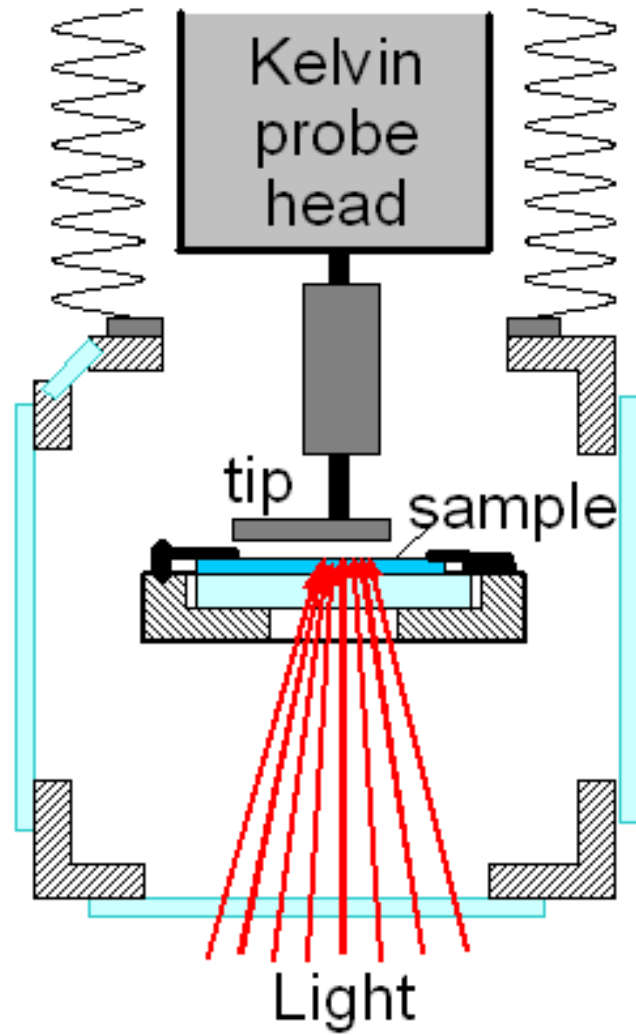


Fig. 2.3: Kelvin probe setup with illumination performed from the backside.

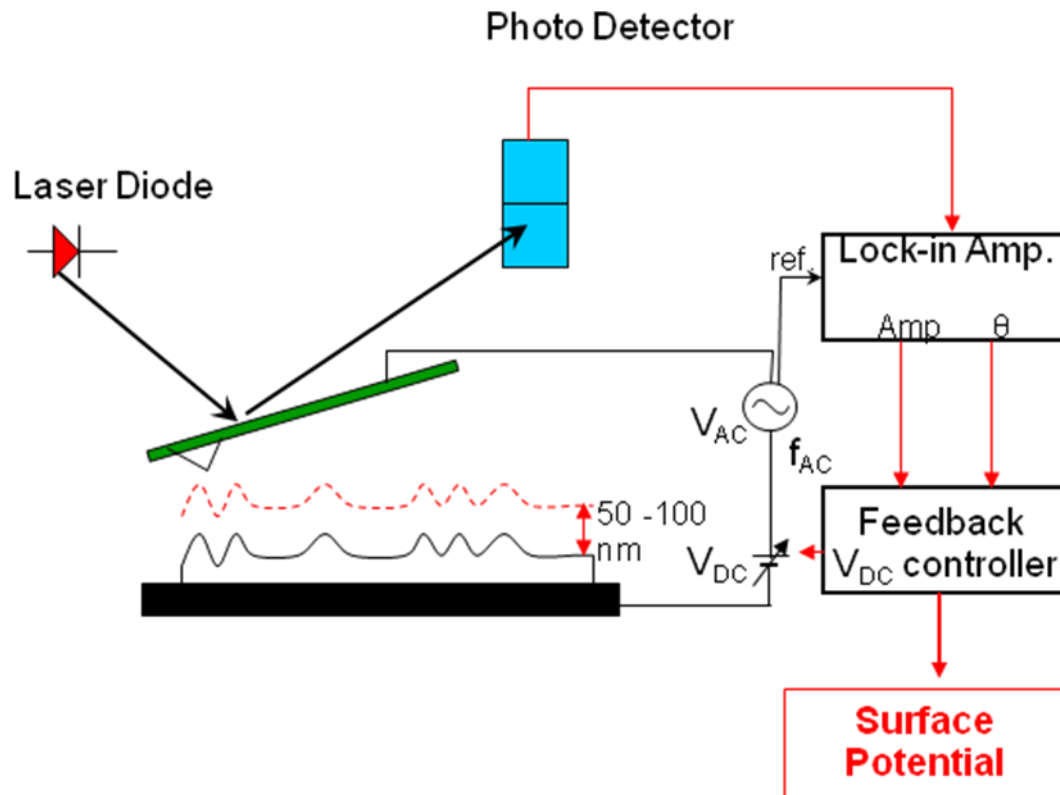


Fig. 2.4: Schematic of Scanning Kelvin Probe Microscope (SKPM).

Chapter 3: Simple Model of Band Bending in GaN

Undoped GaN exhibits approximately 1 eV of upward surface band bending in air ambient.³¹ Band bending is a result of the accumulation of negative charge on the surface. The negative charge on the surface is compensated by the positively charged depletion region. The charge can be located on the surface for reasons including but not limited to surface states, dangling bonds, atoms or adsorbed molecules from the atmosphere, and a thin oxide layer covering the surface of the semiconductor.³² New states can be formed through dangling bonds, impurities and native defects which occur during growth. It has been established that a thin monolayer of chemisorbed oxygen atoms covers the GaN surface, and a thin oxide layer may also be present. This oxide layer has a thickness of ~ 1 nm.³³

The band diagram for a GaN film deposited on a sapphire substrate is shown in Fig 1.3. At the far left edge (the surface), there is a layer of adsorbed oxygen labeled O_2 . Two illumination geometries are shown: front side (from left) and backside (from right). Adsorption of photons causes vertical energy transitions of electrons. If a valence electron located in the depletion region W is excited to the conduction band (CB), then the electron is swept into the bulk. The hole left behind in the valence band (VB) then moves to the surface and reduces band bending Φ_B . There will be almost no recombination of electrons and holes in the depletion region due to the strong electric field on the order of $10^5 V/cm$. Photons captured in the bulk create electron hole pairs which recombine via non-radiative mechanisms or by spontaneous emission of photons, i.e., photoluminescence.

A simple model for band bending at the surface of GaN can be derived. It incorporates the density of negative charge on the surface n_s which causes upward band bending Φ_B . Band bending is related to the depletion region width W through the following relation:

$$W = \frac{n_s}{N_D} = \sqrt{\frac{2\Phi_B \epsilon \epsilon_0}{q^2 N_D}}, \quad (5)$$

where q is the charge of an electron, ε is the dielectric constant for GaN ($= 9.8$), ε_o is the dielectric permittivity in vacuum, and N_D is the concentration of uncompensated shallow donors.³⁴ In this work, the band bending Φ_B will not be directly measured, rather a contact potential difference (CPD) between a probe and our sample will be monitored. The CPD is the difference between two materials work functions and is measured directly by the Kelvin probe. The equation that relates the CPD to band bending is given by:

$$\Phi_B = \phi_m - \chi_s - (E_C - E_F) - qV_{CPD} , \quad (6)$$

where ϕ_m is the work function for the stainless steel probe, χ_s is the electron affinity for GaN, $(E_C - E_F)$ is the energy difference from the Fermi level to the bottom of the conduction band, and qV_{CPD} is the contact potential difference that the Kelvin probe measures. Eq(6) shows that it is sufficient to monitor the contact potential difference to observe changes in band bending. Absolute values of Φ_B can also be estimated from Eq(6), provided that all other variables are known.

The surface photovoltage (SPV) will be used to monitor changes in band bending. SPV is the absolute change in band bending y due to illumination given by:

$$y = \Phi_o - \Phi . \quad (7)$$

Here, Φ_o is the band bending before illumination (dark) and Φ is the band bending during or just after illumination. Although band bending can be changed by photo induced transitions in the bulk, our simple model will neglect these effects.³⁵ It is assumed that the SPV results from changes in the amount of negative charge on the surface. Using Eq(5), the negative charge on the surface can be written as:

$$n_s(y) = \sqrt{\frac{2(\Phi_o - y)\varepsilon\varepsilon_o N_D}{q^2}} = n_s(0) \sqrt{1 - \frac{y}{\Phi_o}} . \quad (8)$$

The negative charge at the surface can be divided into two types: internal (charge at semiconductor surface) and external (oxide layer and adsorbed species). Three major processes occur that will change the amount of negative charge on the surface: emission of

electrons from surface states to the bulk, emission of free electrons from the bulk to surface states, and the accumulation of photo-generated holes at the surface.³²

Increasing the rate of photo-generated holes will increase the SPV. The photo-generated holes can quickly add positive charge to the surface and reduce the amount of band bending. Photons can be adsorbed in the depletion region, bulk or surface states. Adsorption of photons in the depletion region occurs at energies near or above band gap and leads to the creation of electron-hole pairs. Any photons adsorbed in the bulk are expected to give a negligible rise to the SPV. The recombination of electron hole pairs in the bulk will increase the SPV only if the concentration of photo-generated electrons is much larger than the concentration of free electrons in dark. As for the excitation of electrons from surface states, the illumination energy needs to be sufficient enough to remove an electron from surface states over the near-surface barrier into the bulk.

Our simple model will into take account illumination through the backside or the front side of the GaN film. If the sample is illuminated from the backside, adsorption of photons occurs in the bulk region of GaN. The number of photons absorbed in the depletion region per second per unit area is defined as:

$$P_w = \int_{D-w}^D \alpha P_o e^{-\alpha x} dx = P_o e^{-\alpha D} (e^{\alpha W} - 1). \quad (9)$$

Here, α is the adsorption coefficient of the GaN film and P_o is the incident power density in photons per sec per unit area. If the illumination is performed from the front side, the number of photons absorbed in the depletion region per second per unit area is given by:

$$P_w = \int_0^w \alpha P_o e^{-\alpha x} dx = P_o (1 - e^{-\alpha W}). \quad (10)$$

Illumination with photons close to or above band gap creates photo-generated holes in the depletion region. Photons which have energy slightly below the band gap can still create electron-hole pairs due to a photon-assisted tunneling affect that increases the adsorption cross-section in the depletion region (Franz-Keldysh effect). In our model it is assumed that

every photon absorbed in the depletion region creates an electron-hole pair. Therefore, the rate of holes moving to the surface equals P_w . Incoming photons with energy substantially less than the band gap can be captured by surface states. If electrons in surface states absorb sufficient energy to overcome the near-surface barrier, they are swept into the bulk. Illumination of this type reduces band bending and the number of photons absorbed at surface states can be expressed as :

$$P_S = \sigma_{ph}^s n_s P_o e^{-\alpha D} \quad (\text{Backside Illumination})$$

$$P_S = \sigma_{ph}^s n_s P_o \quad (\text{Front side})$$

These emission rates of electrons from the bulk and surface are governed by Boltzmann statistics since they are thermionic transitions. Electrons can either be thermally excited from the surface over the barrier, or they can overcome the barrier and be captured by surface states. These rates are defined as R_{bs} (rate from bulk to surface) and R_{sb} (rate from surface to bulk). The rate of emission from the bulk to surface states is given by:

$$R_{bs} = C_{n1} n N_s^* \exp\left(-\frac{\Phi_0 - y}{kT}\right) = C_{n1} N_C N_s^* \exp\left(-\frac{\Phi_0 + (E_C - F) - y}{kT}\right) \quad (11)$$

where N_C is the effective density of states of the conduction band, N_s^* is the concentration of the semiconductor surface states which can be occupied by electrons, k is the Boltzmann constant, and T is temperature. Electrons from surface states or chemisorbed species can overcome the potential barrier and the emission rate from surface states to bulk is defined by:

$$R_{sb} = C_{n2} n_s N_C \exp\left(-\frac{E_C - E_s}{kT}\right) \quad (12)$$

Here, E_s is the energy level of the surface states in the model where a single energy level pins the Fermi energy and controls the band bending in dark. The constants C_{n2} , C_{n1} in these rate equations can be expressed in terms of the electron capture cross sections, σ_{n1} and σ_{n2} , given by:

$$C_{n1,2} = \sigma_{n1,2} v_n = \sigma_{n1,2} \sqrt{\frac{8kT}{\pi m_e^*}}$$

Here, v_n is the average thermal velocity of electrons and m_e^* is the effective mass of the electrons in the conduction band. Now that the three rates are defined, a total rate equation is defined as:

$$\frac{dn_s}{dt} = R_{bs} - R_{sb} - R^* , \quad (13)$$

where R^* is the rate of photo-generated holes, which is equal to P_w as previously stated. With these rate equations, physical processes that occur during SPV experiments can be defined.

There are three phases in our experimental measurements as follows: 1) turn-on transient when illumination commences, 2) steady state illumination, and 3) decay after illumination ceases. The first and last phases are governed by the same pair of rate equations. The only processes occurring during this period are thermionic ones. The rate when there is no illumination, in dark or post illumination, is given by:

$$\frac{dn_s}{dt} = R_{bs} - R_{sb}$$

Equilibrium occurs when $R_{bs} = R_{sb}$. From this condition, the SPV during the decay is given by:

$$y \approx y_o - \eta kT \ln[1 + b(t - t_1)] \quad (14)$$

$$\text{with } b = \frac{R_o}{\eta kT} \frac{2\Phi_o}{n_s(0)} e^{\frac{y_o}{\eta kT}}$$

where y_o is the amount of band bending at $t = 0$, η is a phenomenological factor, and t_1 is time. From Eq(14) it is seen that the band bending after illumination decays as a logarithm of time. The rate equation that governs the SPV transients can be rewritten accounting for Eqs. (9), (11), (12) as

$$-\frac{n_s(0)}{2\Phi_o \sqrt{1 - \frac{y}{\Phi_o}}} \frac{dy}{dt} = R_o \exp\left(\frac{y}{\eta kT}\right) - R_o \sqrt{1 - \frac{y}{\Phi_o}} - R^* , \quad (15)$$

An equilibrium is reached when $R_{bs} = R_{sb} - R^*$; this yields the maximum possible photovoltage during illumination. Equation (15) can be solved for this photovoltage and is given by

$$y_o = \eta kT \ln \left(\frac{cP_o}{R_o} + 1 \right) \quad (16)$$

where

$$R_o = C_{nl} N_c N_s^* e^{\left(\frac{\Phi_o + E_c - F}{kT} \right)}.$$

η is a phenomenological factor which is analogous to the non-ideality factor in Schottky diode theory. In the above approximation it is equal to unity, but in other models it can vary from 0.5 to 2.³⁶ From Eq(16) it is deduced that there is a linear and log dependence of photovoltage on light intensity. If the intensity is $cP_o < R_o$, then there is a linear dependence. If $cP_o > R_o$, then there is a logarithmic dependence.

It has been proposed that the environment might affect SPV during illumination through photo-induced absorption or desorption of surface species. In this simple model these effects are not included explicitly but their effect can be revealed indirectly. In this thesis, measurements of SPV transients and steady state values were performed in a variety of environments, as well as a wide range of photon energies. A comparison between the model and experimental data will be performed and discussed.

Chapter 4: Surface Potential Measurements of GaN

4.1 Spectral Response

Important information about surface states in GaN can be obtained from analyzing the surface photovoltage. The first data analyzed was the photovoltage response as a function of photon energy. These data give information about the location of surface states and their capture cross-sections. The SPV spectra for undoped and Si-doped GaN samples are shown in Figs. 3.1 and 3.2, respectively. In undoped GaN there is a threshold for the SPV signal around 1.25 eV photon energy and a maximum SPV occurs at 3.4 eV, which is close to the band gap of GaN (3.42 eV at RT). As the photon energy becomes greater than the band gap, there is a decrease in the SPV signal. This decrease is due to the fact that most of the photons are absorbed in the bulk and not in the depletion region. Our model predicts that the SPV should become zero once photon energies exceed the band gap energy. Instead, it does not go to zero and an SPV of about 0.38 eV is still observed. This is caused by absorbed photons in the bulk that are re-emitted via PL and then become absorbed in the depletion region. Also, for vacuum conditions it is noted that the SPV is slightly decreased at energies less than 2.2 eV and increased above 2.4 eV. In Si-doped GaN there is a threshold energy around 1.7 eV and a maximum SPV of 0.45 eV occurs at 3.35 eV photon energy. Again, after the bandgap energy is exceeded, the SPV drops below its maximum value and is approximately 0.2 eV. This sharper decrease can be attributed to the narrower depletion region in this doped sample, which reduces the probability of PL photons reaching the depletion region and becoming absorbed.

Using the SPV spectra, the absolute value of band bending can be calculated and has been done so for the undoped sample. Using the $y_o(P_o)$ dependence and varying the model in a wide range of their reasonable values, an estimate for the absolute value of band bending is $\Phi_o = 0.9 \pm 0.3 \text{ eV}$ at 295 K. This is in excellent agreement with the predicted values for the absolute value of band bending. Since 365nm (~3.4 eV) light provides the greatest photovoltage signal, this wavelength will be used for most of our measurements.

4.2 Intensity Dependence

Typical SPV transients are shown for below-bandgap light are shown in Fig. 3.3. As expected, the SPV rise with time was slow at very low illumination intensities. At higher intensities the SPV increased more steeply and required less time to achieve saturation. The decay of the SPV was slow no matter what light intensity was used. To ensure that no accumulative effects were present during these experiments, the SPV was measured at select light intensities and photon energies after dark conditions were achieved and were not achieved. The signal for the same illumination intensity and energy was reproducible.

Figure 3.4 shows the steady-state surface photovoltage dependence on light intensity for selected photon energies. At very low illumination intensity, an extended illumination time is required to reach nearly complete saturation of the SPV. Data for intensities between 10^8 and $10^{10} \text{ cm}^{-2}\text{s}^{-1}$ required durations up to 1 h using 365 nm illumination. All energies used show a logarithmic dependence on the illumination intensity. Using these values the intrinsic band bending is estimated to be $\Phi_o = 1.1 \text{ eV}$, assuming that 2% of the light is absorbed in the 150nm wide depletion region with $D = 2.5 \mu\text{m}$, $n_s = 7 \times 10^{11} \text{ cm}^{-2}$, and $N_D = 4 \times 10^{16} \text{ cm}^{-3}$. This value is consistent with the largest photovoltage observed in Fig. 3.4 (around 0.6 eV) and is in agreement with previous reports.³⁷ An interesting effect is observed at high intensities of band-to-band light. In air ambient at the highest light intensity and energy, the SPV reached a maximum of 0.62 eV in the first few seconds and then decreased by almost 0.3 eV under UV exposure for 3 hours. This quenching effect decreases with light intensity and could not be observed for $P_o < 10^{-3} \text{ W/cm}^2$.

4.3 Effect of Environment

The effect of the environment on SPV has also been studied with experiments performed in air, vacuum, nitrogen and oxygen. In our experimental set-up, the cryostat was evacuated using a turbo pump and gases were then introduced, as shown in Fig. 3.5. Changing the environment to nitrogen or oxygen was done using a pump-purge process, where the system

was pumped down to mid-vacuum (10^{-4} mbar) and then purged to 1 atm using a gas tank with the pump valved off. This procedure was repeated three times to reduce contamination due to other gas molecules or water vapor.

SPV measurements on the undoped sample GaN750 are shown in Fig. 3.6. for air, vacuum, and nitrogen environments. In air ambient during illumination, an instantaneous increase in SPV is observed; however, under continuous illumination there is a decrease in the SPV over time. This decrease corresponds to an increase in band bending, or an increase in the surface negative charge. It is hypothesized that oxygen is chemisorbed to the GaN surface during illumination (photo-induced adsorption). Ambient or physisorbed O_2 molecules strongly bind to the surface when bulk electrons are excited over the surface barrier and bind to the O_2 . In contrast, under UV illumination in vacuum an increase in SPV is observed over time, likely due to the desorption of some negative surface species (photo-induced desorption). In this case, surface species are photo-dissociated and desorb in the low pressure environment. This process reduces the amount of negative charge on the surface, thus giving rise to a decrease in band bending. Lastly, SPV measurements in N_2 indicate a slight decrease in SPV over time. This decrease was not as large as for the air ambient and was most likely due to impurities. Measurements were repeated with the Si-doped sample GaN595 and an oxygen environment was included (see Fig 3.6). The nitrogen measurement shows no decrease in SPV and looks similar to vacuum. A measurement in an oxygen environment showed the largest decrease in SPV during continuous UV illumination. Oxygen therefore plays a major role in the decrease of SPV observed during continuous illumination with 365nm light. It should be noted that sample properties can change after extended periods of UV illumination and further investigations are necessary.

4.4 Photoluminescence Measurements

To verify that the SPV decrease during continuous UV illumination was not some artifact of the Kelvin probe investigations have also done using a photoluminescence setup. An

experiment was done measuring the PL intensity in air. Figure 3.7 shows the results of these measurements, where the observed PL signal decreases with time. The PL signal received depends on the width of the depletion region. During illumination the PL signal decreased, corresponding to an increase in band bending. Measurements were also performed in vacuum showing a relatively constant PL signal after an initial increase. These results verify the effect observed with the Kelvin probe.

4.5 Decay of SPV

The SPV decay after ceasing illumination is shown in Figs.3.8 and 3.9 for the undoped GaN sample. Figure 3.8 shows SPV decays for various exposure times and environments. All measurements decay nearly logarithmically with similar rates in vacuum and air ambient. However, after prolonged exposure, the SPV signals in vacuum and air decayed in substantially different manners. In vacuum, the decay is very slow and the dark signal cannot be reached even after several days. In air, the SPV signal drops from 0.4 to 0.2 eV in about 5 s and then decays nearly logarithmically to reach its dark value in about an hour.

The decay behavior after intense illumination shows rates much slower than the rates predicted by Eq(14). Agreement with our calculated curves is good at lower energies (580 nm, 1000 nm) but begins to fail for energies above 440 nm. Further investigations were performed at higher energies to see if the wavelength or intensity causes the discrepancy. Only by lowering the intensity of the band-to-band light could agreement between our model and experiment be improved. The largest discrepancy was observed at 365nm and full illumination power. This discrepancy can be resolved if one assumes that processes such as chemisorption or charge transfer to/from the surface occur at sufficiently high intensity.

4.6 Effect of Temperature

The absolute value (or baseline) of the contact potential difference decreased by 0.15 eV as the sample temperature was increased from 295 to 400 K in vacuum. This indicates that upward band bending at the surface was increased by this value. Measurements were not

performed in ambient as to not contaminate the cryostat with water vapor. The maximum SPV at 400 K was increased from 0.64 eV to 0.72 eV. A comparison of the decay signal after illumination for 295 and 400 K can be seen in Fig 3.10. At 400 K, the decay of the SPV signal can be described by our model, but the slope is steeper than expected. This discrepancy may indicate that the mechanism for the decay of band bending may be more complicated than our model predicts.

Chapter 4 Figures:

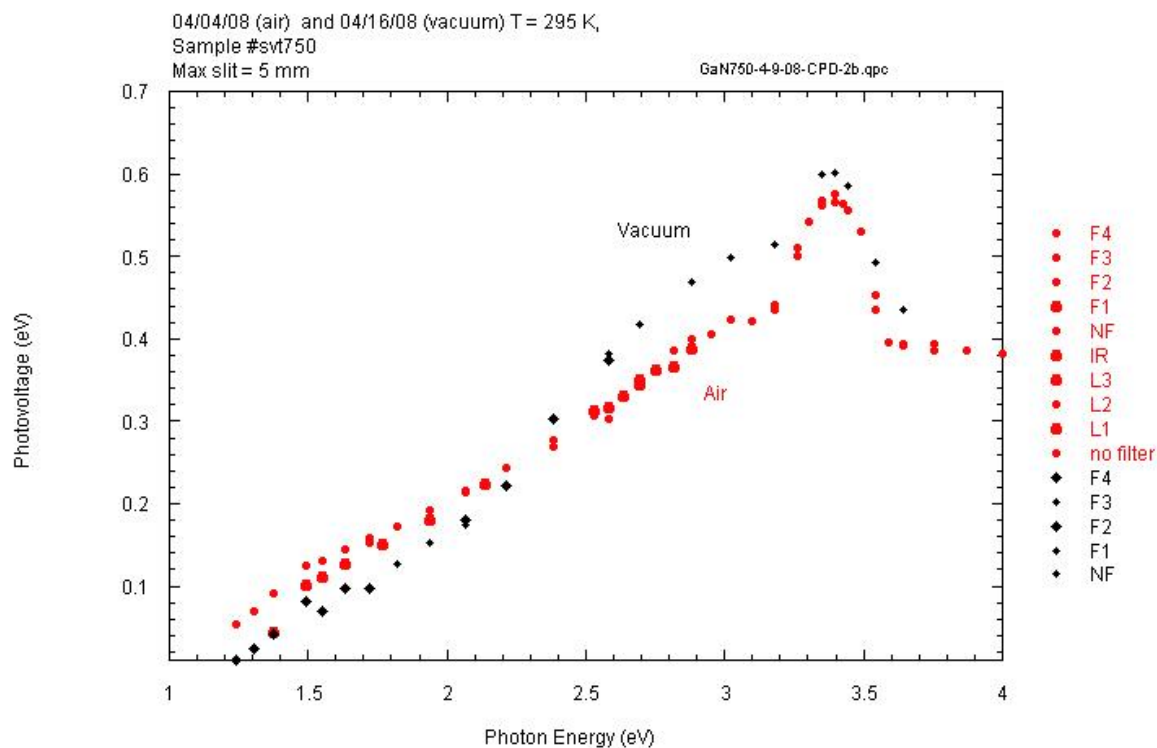


Fig. 4.1: Steady-state photovoltage spectrum for undoped GaN750 at 295 K in air ($P = 6 \times 10^{16} \text{ cm}^{-2} \text{ s}^{-1}$).

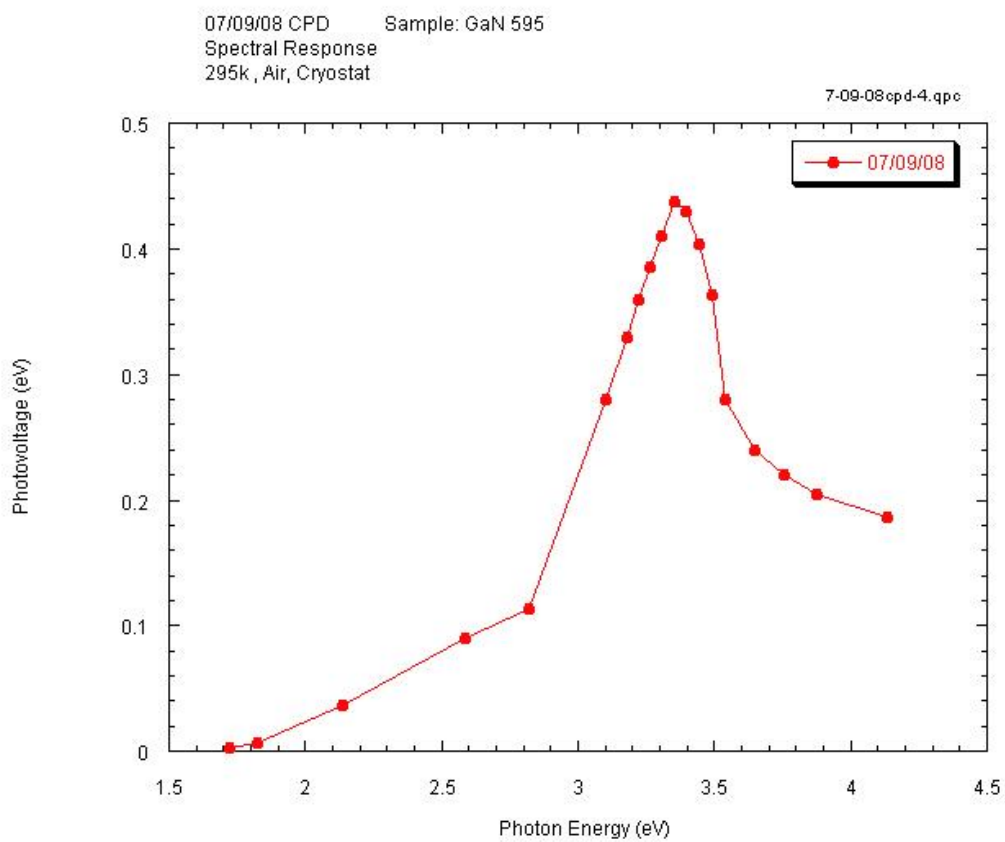


Fig. 4.2: Steady-state photovoltage spectrum for Si-doped GaN595 at 295 K in air ($P = 6 \times 10^{16} \text{ cm}^{-2} \text{ s}^{-1}$).

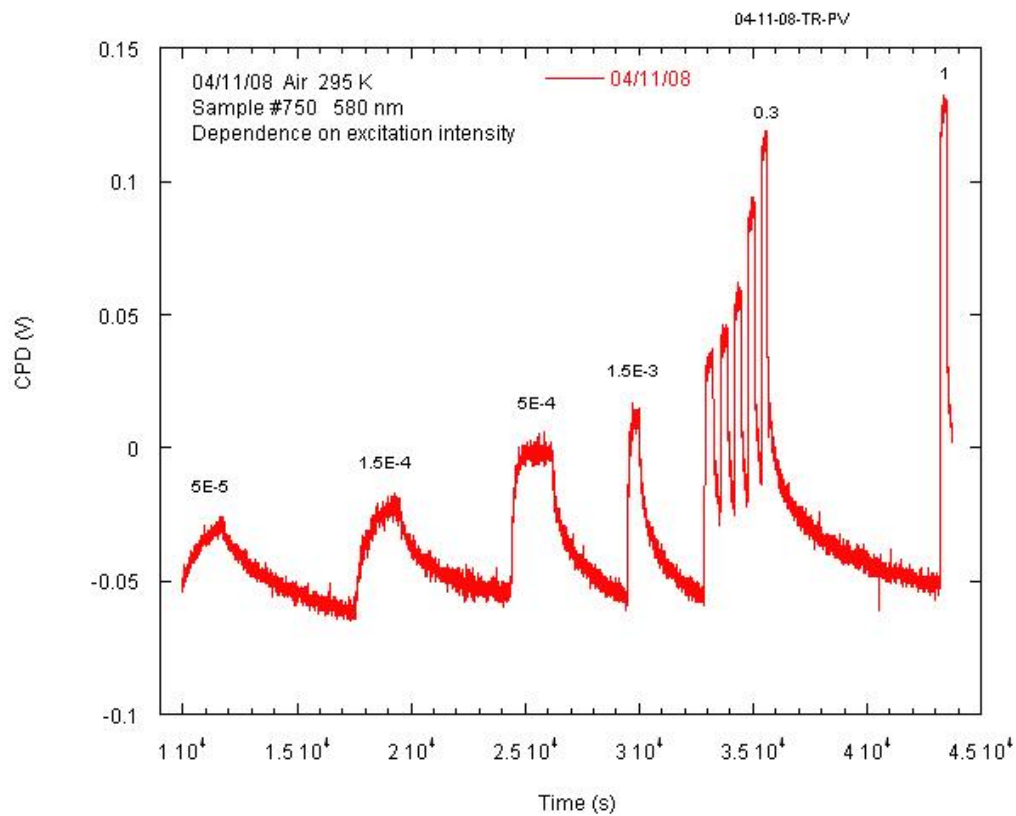


Fig. 4.3: CPD transients (RT, air) obtained with illumination at 580 nm with various intensities.

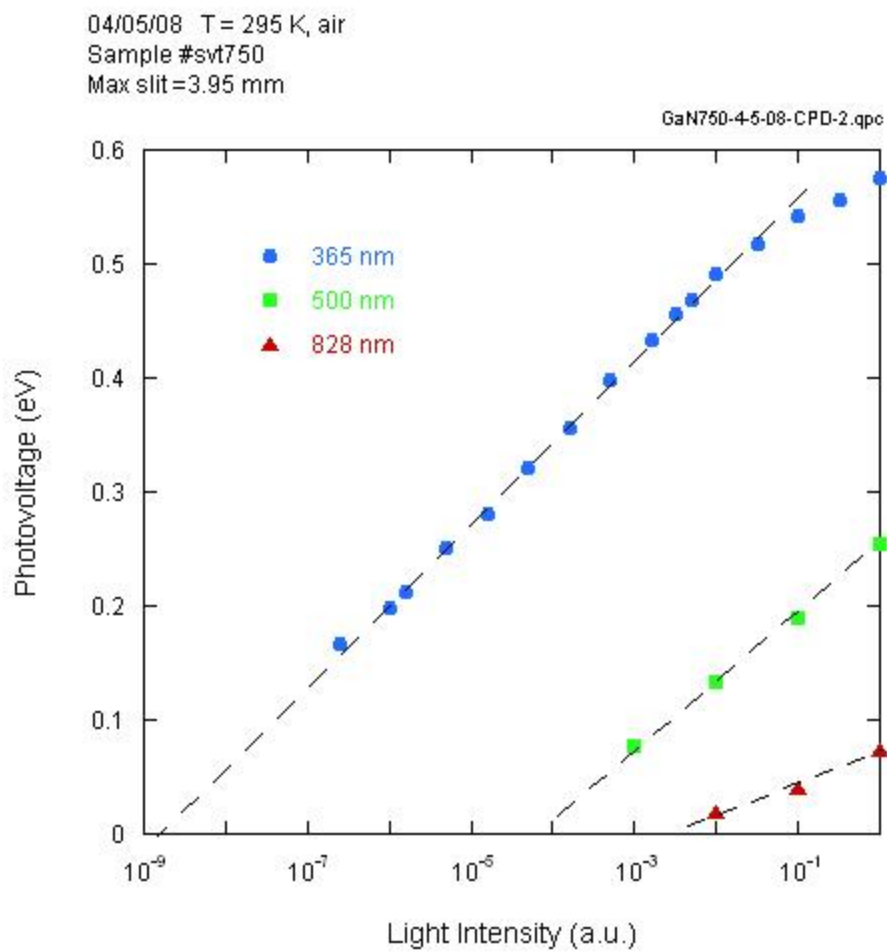


Fig. 4.4: Dependence of SPV saturation on light intensity at 295 K in air.

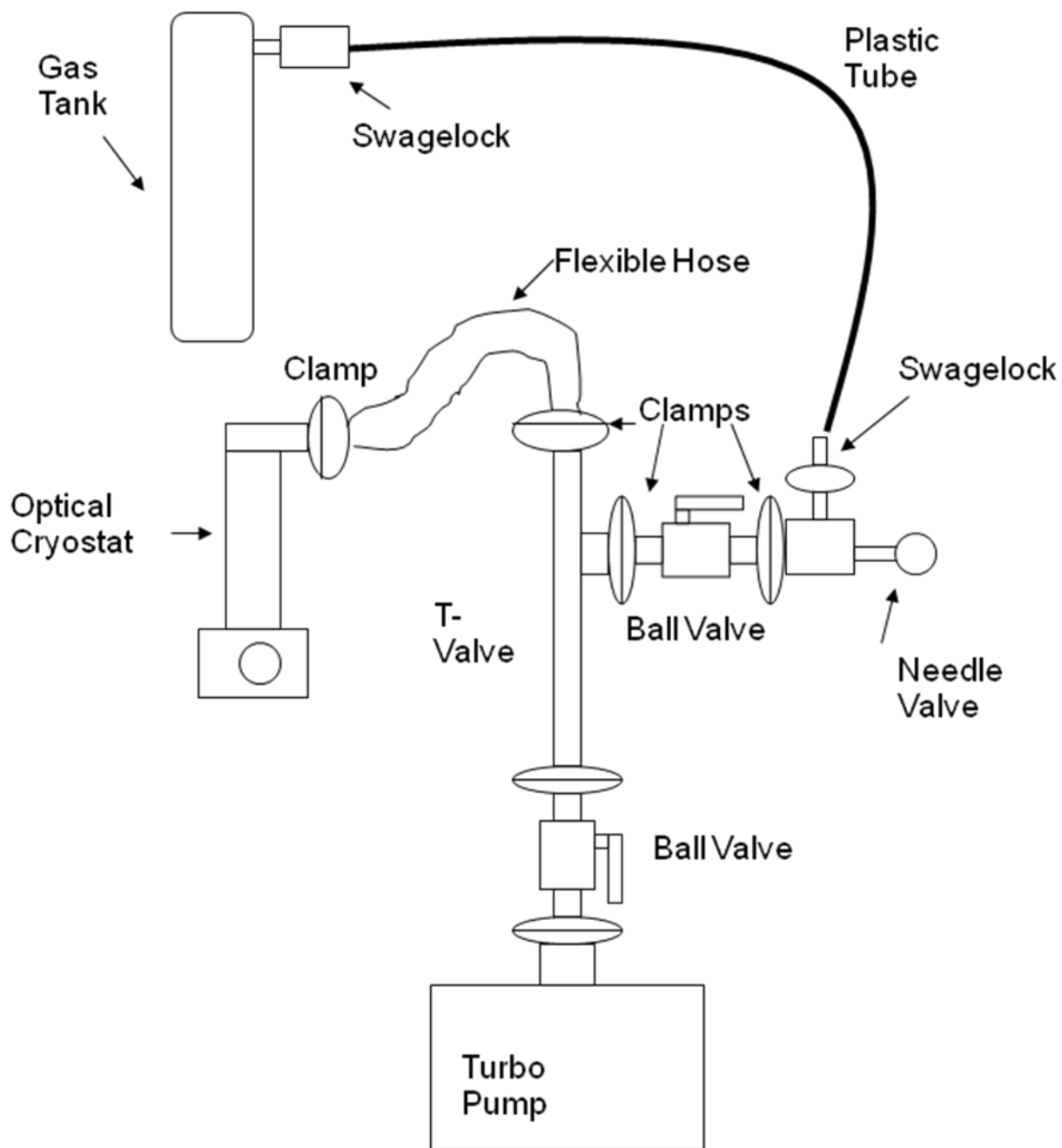


Fig. 4.5: Schematic of pump-purge system.

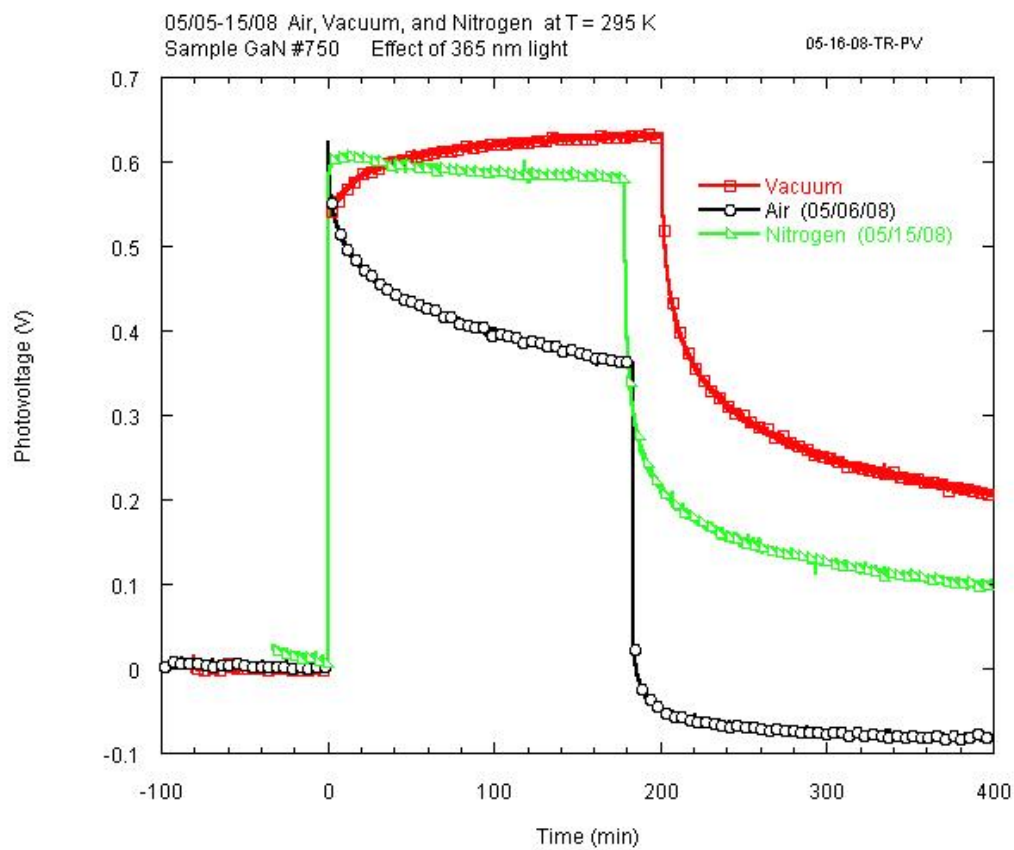


Fig. 4.6: SPV steady state behavior as a function of environment for GaN750.

6-19-08 / 2/28/09 CPD Sample: GaN 595
1 hour base ~1 hour 365 expose ~2 hour relax
Original Dark CPD -0.105 V (air), -0.111 V (O)
295k, Air, oxygen, Cryostat

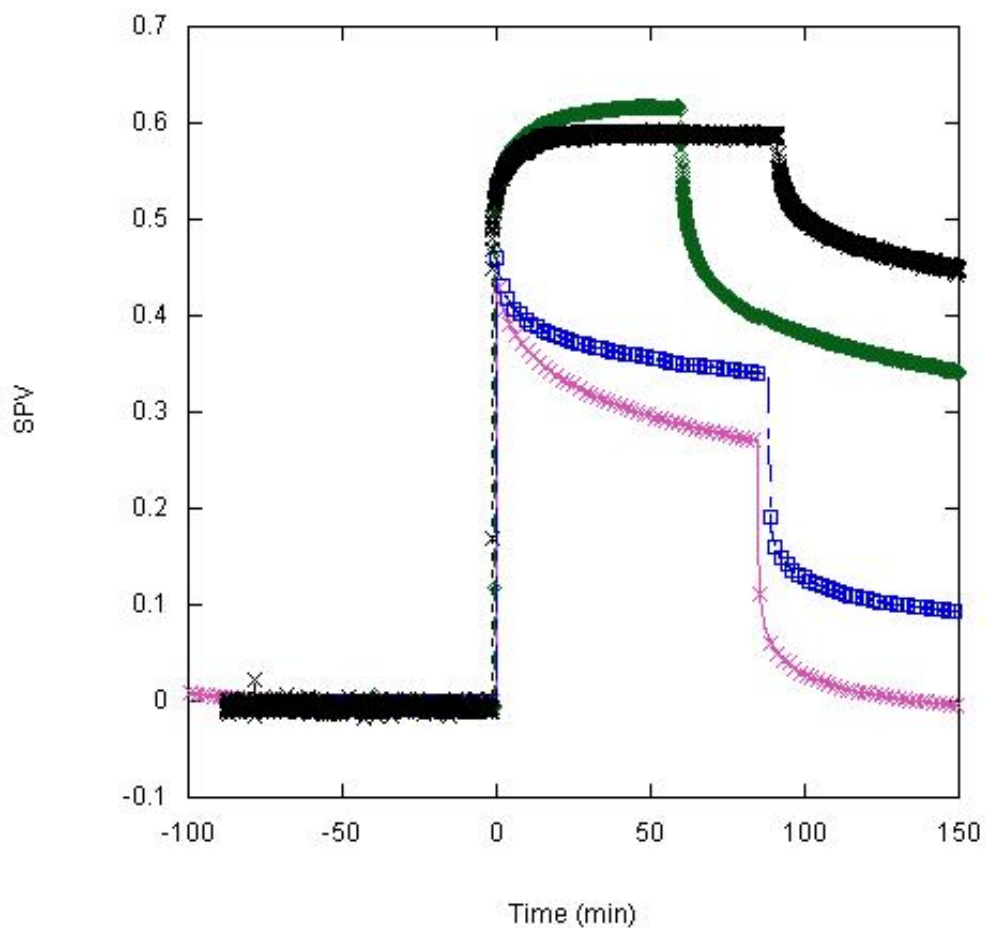
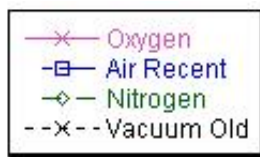


Fig. 4.7: SPV steady state behavior as a function of environment for GaN595.

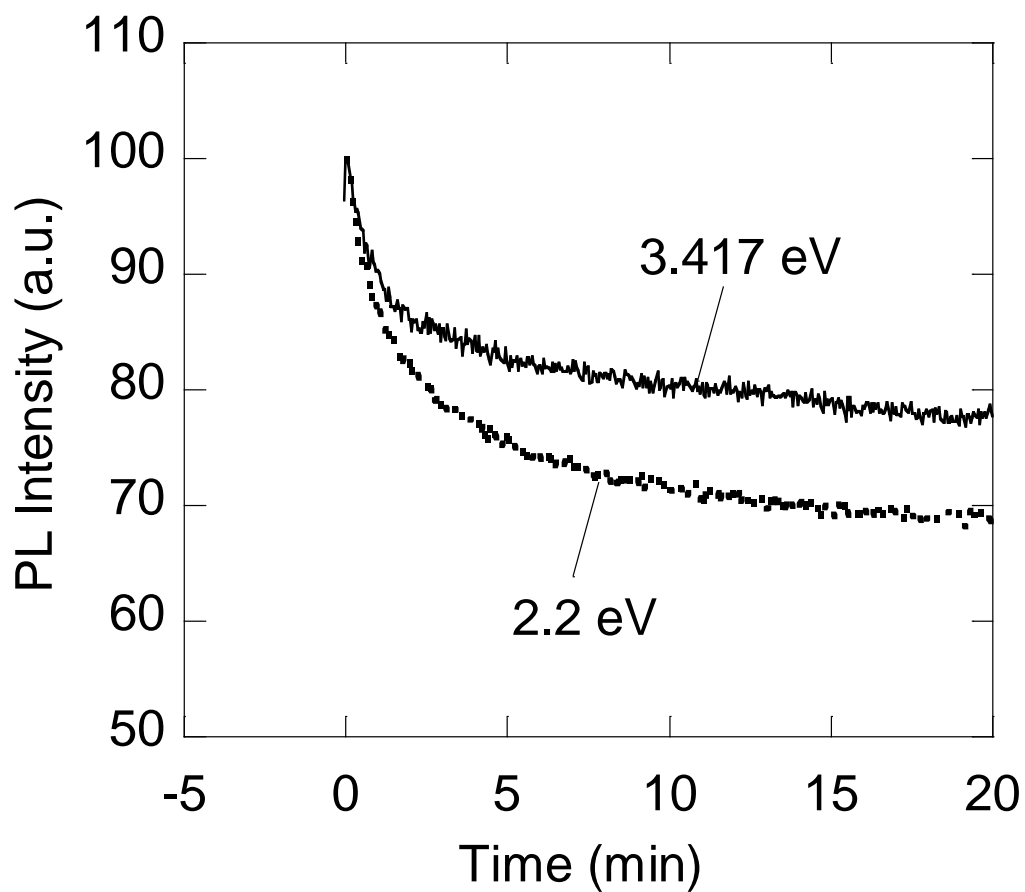


Fig. 4.8: Evolution of PL intensity for GaN750 in air under continuous exposure (HeCd laser).

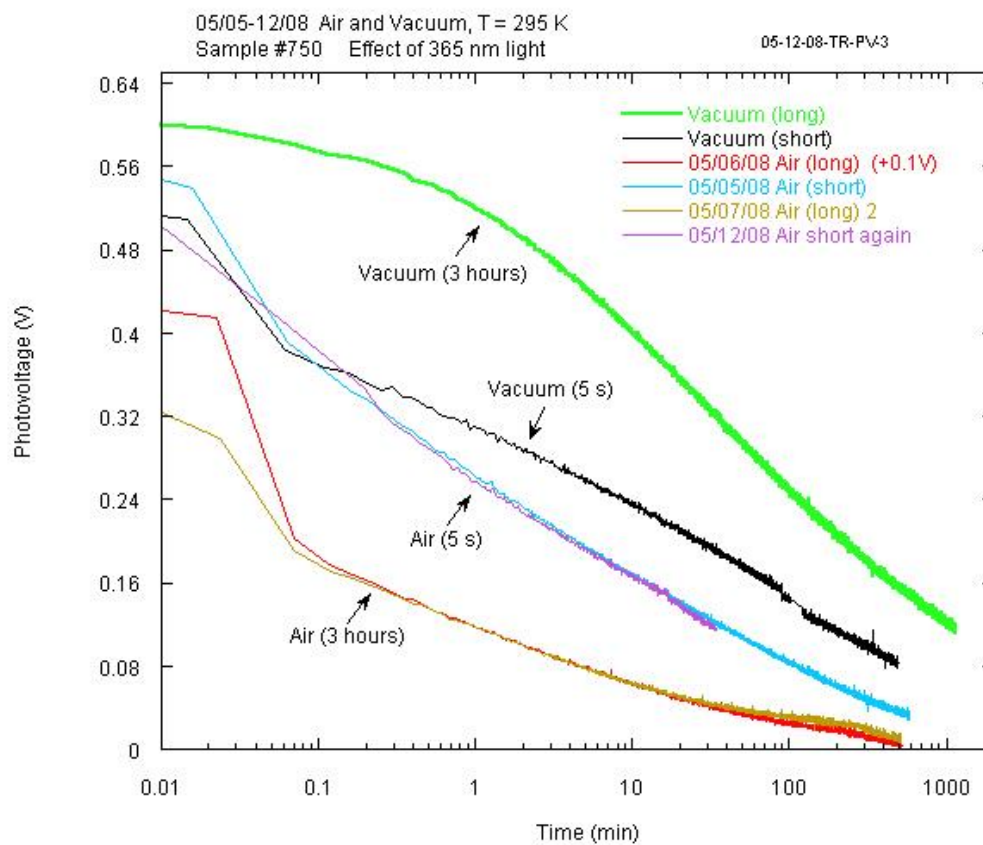


Fig. 4.9: Decay rates shown for GaN750 after illumination with 365 nm light for different exposure times and environments.

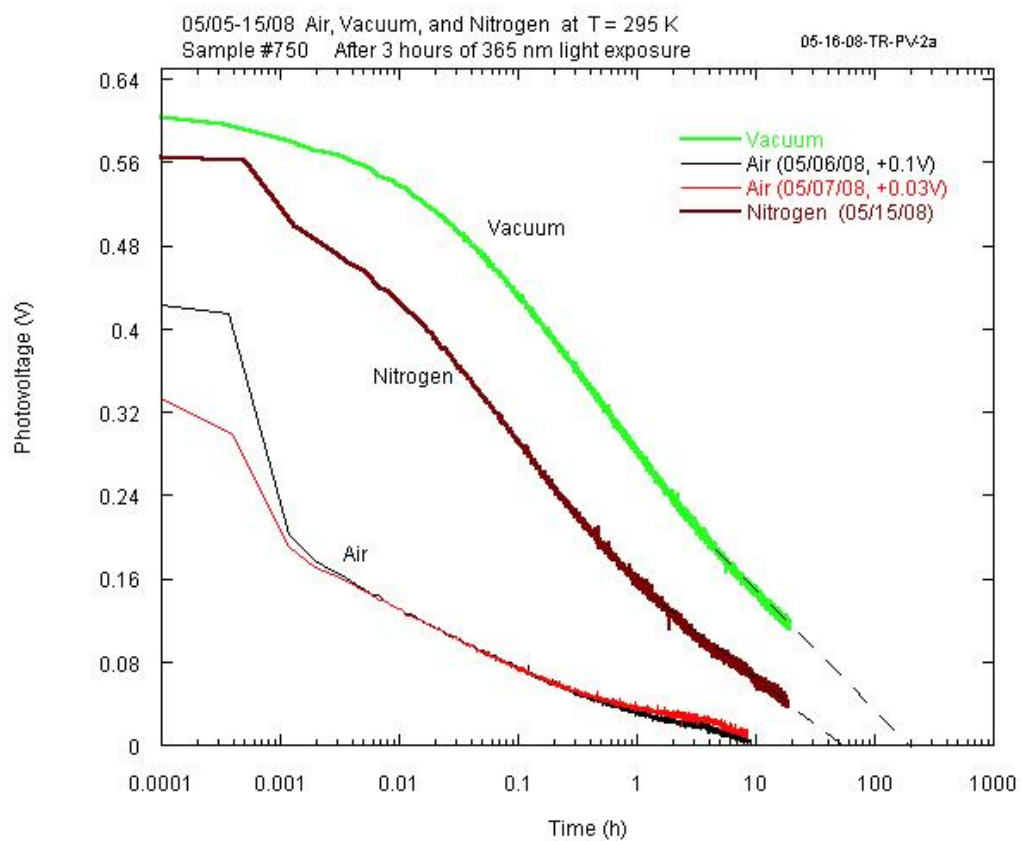


Fig. 4.10: Decay rates for GaN750 under different environments at 295 K (~3 h exposures).

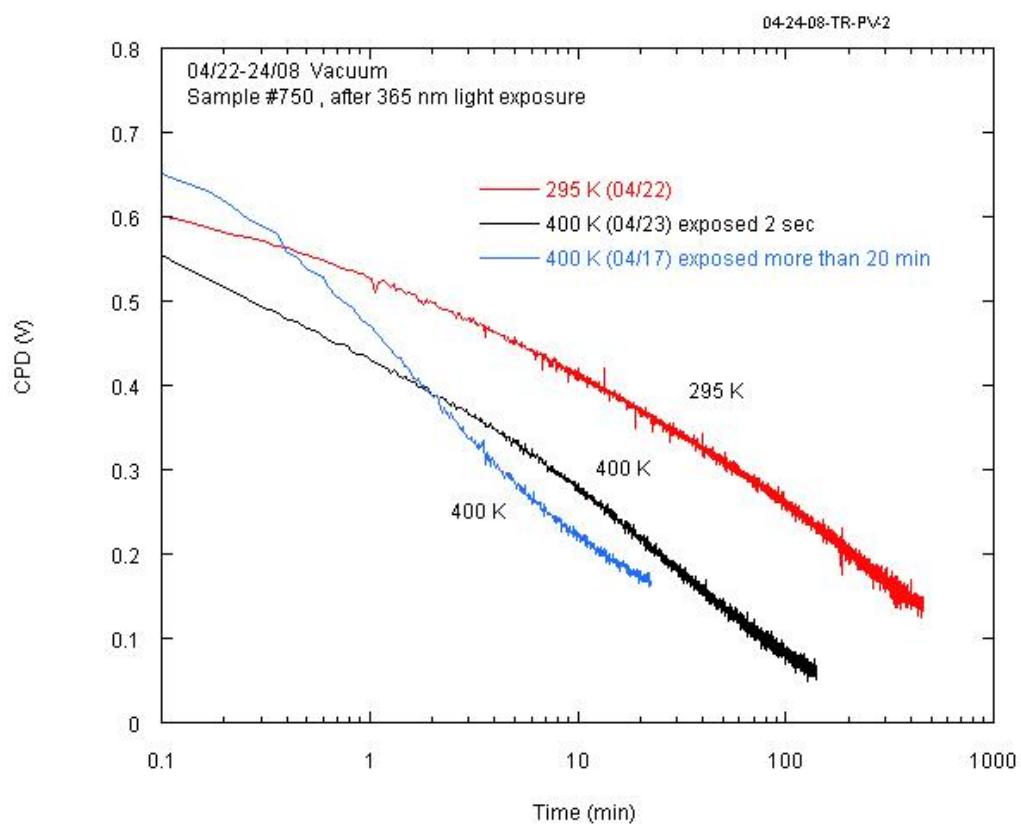


Fig. 4.11: Decay rates shown for GaN750 under vacuum at 295 and 400 K.

Chapter 5: Conclusions

Extensive investigation of the SPV for an undoped n-type GaN film has been done with a Kelvin probe. Measurements have been performed in different environments (air, nitrogen, vacuum), as well as at 295 and 400 K. The observed dependence of the SPV on illumination intensity, as well as the transients of SPV when illumination is ceased with band-to-band and below-bandgap light, is explained consistently with a simple model. The model accounts for transfer of electrons from surface states to bulk and back, as well as the accumulation of photo-generated holes at the surface. The upward band bending in dark was estimated to be $\Phi_o = 0.9 \pm 0.3 \text{ eV}$ at 295 K. Illumination with photons which have energy close to the bandgap reduce band bending by up to 0.64 eV at 295 K and 0.72 eV at 400K in vacuum. Very slow decay of SPV observed in dark after ceasing illumination is explained by the transfer of electrons from the semiconductor surface states to an oxide layer and to adsorbed species, which results in the conversion of physisorbed species to chemisorbed ones. A Si-doped n-type GaN film was also investigated in this study. During illumination with band-to-band light, the SPV decreased over time for this sample as well as the undoped one. Measurements show that this behavior is most likely due to the photo-induced chemisorption of oxygen species on the surface.

Appendix

How to use the Kelvin Probe

The first thing to do is to determine what kind of measurement you will be taking. Depending on that will change how you are going to set the system up. IT ALSO REALLY HELPS TO READ THE KELVIN PROBE MANUAL. It is well written and packed full of useful information.

Key points on the set up:

- Turn on the lamp 5-10 minutes early so that it has ample time to warm up.
 - Sometimes when you turn on the lamp it will crash your cpd reading. To fix this there are two options. First one is to remember the DCO you are at. Set the DCO to 1.000 and then back to its original value.
 - This should be fixed though as of 1-12-09. The problem arose from the KP control box being too close to the power supply. They interfere with each other somehow and the control box was moved above the computer.
- If you are doing a single wavelength of light, go ahead and set the slit widths before hand. There is handout with an excel table that will tell you what slit widths to use with what wavelengths and filters. Remember that a full turn is .5 mm, try to be pretty accurate with the slit sizes.
- Make sure to have done a sufficient baseline! The CPD should be pretty stable over 30 minutes to 1 hour. If you are seeing changes of around .05 you should probably wait longer before taking a measurement.
- Write down the pressure, temperature, and humidity in the log book along with the important KP settings. These values affect the CPD and its good to notice trends.

Here is a quick How to Operate the KP (screen capture at end):

- Make sure Frequency = 100, Amp = 25 DCO = between .5 - .3
- We will assume that the sample is loaded and ready to go. Once the sample is loaded you want to take the socket wrench and approach the tip to the sample. This could take a few turns or a lot of turns so be patient. To tell how close you are to the surface you want to watch the gradient. The gradient should be close to zero or close to it, $-+$.004 when you are nowhere near the sample. When you start approaching and you get around .015 that's when you want to slow down. The numbers are going to change slowly at first but once you get going they change dramatically. There is a piece of paper on the table that will tell you which way to turn the wrench.
- The next thing to do is to do the fine adjust. This is done with the DCO. The DCO is a fine adjustment and it will bring the tip closer to the surface very slowly. When you are physically taking measurements you want the DCO to be as close to zero as possible. This is going to involve backing out, using the wrench some, and changing the DCO. It is a time consuming process and takes practice. You want to have the $DCO < .1$
- After this set your pretty much ready to get your baseline, illuminate, and go!

Attached is a screen capture of the KP software during data collection. An explanation of the symbols will be given.

A:

There are 3 settings here that are very important.

Frequency – rate at which the KP tip oscillates back and forth, we do not want to keep this value very close to the resonant value of the tip. Something between 100-120 works best we found.

Amplitude – how large the oscillations of your KP tip will be. Be careful if you are changing these settings while you are approached. You would cause the tip to oscillate INTO the sample if you are too close. It is recommended you pull away from the sample while changing the amplitude.

DC offset – This is a fine approach towards the sample. We want this to be as close to zero as possible. The best way I have found to set it is:

When you start your coarse approach set your DCO to .5 - .3 then go ahead and do your course approach till you have a gradient between .010 - .030. Then go ahead and bring your DCO down until you have the desired gradient. If these settings do not work simply retract the probe and adjust them.

B:

There are 2 settings here it is important to note:

A/D Points and A/D Rate. These 2 settings are going to control the rate at which you take data. The main thing to note here is that the CYCLES is dependent on these two settings. In the manual it says that the cycles should be an INTEGRER number larger than 15.

C:

There are 3 settings here to take note of

Number – this is the number of measurements the probe is going to take before cutting off. If you set this to zero, it will take measurements until you hit stop.

Average over – This is how many points the KP will take the average of. We have used anything between 5 and 10 in the past. At 10 measurements per average, it takes about 3 seconds per data point which isn't too bad.

Interval – The amount of seconds between successive measurements. When we are looking at the transience I usually leave this at zero until I am ready to leave the experiment overnight. Then I will usually set it to 20-30 to reduce the amount of measurements since nothing is changing rapidly. You can also increase this to 5-10 for baseline measurements while you wait. It is good to keep it at 0 though if you expect any great change in the cpd.

D:

These buttons up top are controllers for the program I will explain what each means.

The first button that looks like an excel chart - This button will start filling in the data table if pressed. Otherwise it will keep overwriting some point. The data table will go up to 1000 points and then automatically save if the disk button is pressed in.

Disk Button – This is pretty much your AUTO save button. What it will do is save your data file in the format you want then start a new file. If you look at letter **E** it will show you the saving format.

Feet – This enters you in tracking mode which will adjust the DCO to keep the gradient constant, more in section F.

The pink clock – If you have this button pressed, every time you hit GO it will reset the time in the data table back to zero and start counting up. We usually use this every time we start a new measurement.

SIDE NOTE

Now when you open these files in excel you will get a data table that has 1000 rows. Make sure when copying the data that you **DO NOT TAKE THE LAST ROW**. There is an error when the program saves the data that it does not overwrite the last data point. So the last data point should be the first data point in your file. We usually ignore this data point since our graphs usually have thousands of data points.

F:

Tracking mode: Now there are 3 settings

Set Point Gradient - What value do you want the gradient to be. The program knows that the gradient is going to be a negative number so there is no need to enter the negative sign. Make sure you pick a gradient around .3. It might be more or less depending on the sample. You want something stable that won't crash from a slight bump or anything.

Step Size – This is how much the DCO is going to change per measurement if the gradient is not close enough to the set point.

Max Gradient Deviation – You can set this to whatever you want, but it is going to be the largest value that the gradient can be away from the set point before it stops changing the DCO. I usually give this some leeway so that the DCO is not changing every measurement.

The screenshot shows the KP6500 Control Program interface. At the top, there are menu options: File, Display Controls, Controls, Configure, Windows, and Help. Below the menu is a toolbar with icons for various functions.

Probe Controls Panel (A): Contains settings for Frequency (1050.0), Amplitude (25), DC Offset (0.036), Backing Potential Controls (Upper BPMV: 0.600, Lower BPMV: -0.400), Scan Steps (1), Data Acquisition Controls (Trigger Delay: 151, Auto), A/D Points (1024), A/D Rate (5976), and D/A Delay (35).

Table (D): A data table with columns: n, Time (s), CPD (V), Error (V), and Gradient. The data rows are as follows:

n	Time (s)	CPD (V)	Error (V)	Gradient
157	1008.550	-0.132	0.000	-0.250
158	1012.630	-0.131	0.000	-0.250
159	1017.130	-0.131	0.000	-0.250
160	1021.030	-0.131	0.000	-0.250
161	1024.950	-0.131	0.000	-0.250
162	1028.940	-0.131	0.000	-0.250
163	1033.010	-0.130	0.000	-0.250
164	1036.760	-0.130	0.000	-0.250
165	1040.550	-0.132	0.000	-0.250
166	1044.610	-0.132	0.000	-0.250
167	1049.420	-0.131	0.000	-0.250
168	1053.190	-0.132	0.000	-0.250
169	1058.140	-0.131	0.000	-0.250

Raw Signal Plot (F): A graph showing Amplitude (V) on the y-axis (ranging from -0.01 to 0.06) versus Points on the x-axis (ranging from 93 to 1023). The plot displays a series of green rectangular pulses.

File Save Setup (E): A dialog box for saving files. It includes fields for File Name Options (Filename root: KP6M, Ext: .index, Time format: ddhhmmss), File Save Method (Time based), and Default data Path (C:\Program Files\MTS\KP6500).

Tracking Mode (F): A dialog box for tracking options. It includes Set Point Gradient (0.250), Step Size (0.001), Max Gradient Deviation (0.003), and buttons for Begin and Stop.

Latest Readings: Shows CPD (V) as -0.131 and Gradient as -0.250. A Low Pass Filter is set to Sigma 0.001.

Bottom Status Bar: Shows the file path C:\Program Files\MTS\KP6500\15125606.CPD, the start button, and the time 1:06 PM.

KP-6500 Control Program

File Display Controls Configure Windows Help

1.0

KP-6500 Co...

Probe Controls

Frequency 105.0

Amplitude 25

DC Offset 0.036

Backing Potential Controls

Upper BPFM 0.600

Lower BPFM -0.400

Scan Steps 1

Data Acquisition Controls

Trigger Delay 151

A/D Points 1024

A/D Rate 5976

D/A Delay 35

Series Controls

Number 0

Average over 10

Interval (s) 0.000

n	Time (s)	CPD (V)	Error (V)	Gradient
157	1008.550	-0.132	0.000	-0.250
158	1012.630	-0.131	0.000	-0.250
159	1017.130	-0.131	0.000	-0.250
160	1021.030	-0.131	0.000	-0.250
161	1024.950	-0.131	0.000	-0.250
162	1028.940	-0.131	0.000	-0.250
163	1033.010	-0.130	0.000	-0.250
164	1036.760	-0.130	0.000	-0.250
165	1040.550	-0.132	0.000	-0.250
166	1044.610	-0.132	0.000	-0.250
167	1049.420	-0.131	0.000	-0.250
168	1053.190	-0.132	0.000	-0.250
169	1058.140	-0.131	0.000	-0.250

Raw Signal

Amplitude (V)

Points

Autoscale Manual Scale: Max 0.074 Min -0.027 UBP LBP Power Spectrum

File Save Setup

Header Information Lines

File Save Method

Root based Time based Ask user

File Name Options

Filename root KP6500

Next index 0000

Time format ddhhmmss

Default data Path C:\Program Files\MTS\KP6500

Default Data Format 0.000

Tracking Mode

Tracking Options

Set Point Gradient 0.250

Step Size 0.001

Max Gradient Deviation 0.003

Begin Stop

Latest Readings

CPD (V) -0.131

Gradient -0.250

Low Pass Filter Sigma 0.001

File written as C:\Program Files\MTS\KP6500\15125606.CPD

start

XP6500

XP6500 Control Progr...

KaleidaGraph

1:06 PM

Focus your tip and surface as usual after loading your sample. You should make sure that the room is dark!!!! Ambient light can increase the SPV by 0.1-0.2 eV and throw off your measurements. The light inside the AFM however does not affect the SPV.

Start your SKPM measurements. To do this make the scan size zero, and disable slow axis scanning. Make the scan size zero to make sure that you are scanning the same spot. Now you need to play with the drive frequency enable SKPM on the Dimension IIIa. You also need to make sure that the tip is biased, which it should be, and that the Interleave settings are set to lift.

When doing these measurements make sure to take a sufficient baseline! Also when illuminating try to keep the illumination intensity constant. Changing it could affect the SPV measurements.

The image below shows the normal SKPM settings

The screenshot displays the NanoScope Control software interface with the following settings:

- Scan Controls:**
 - Scan size: 0.00 nm
 - Aspect ratio: 4:1
 - X offset: 0.00 nm
 - Y offset: 0.00 nm
 - Scan angle: 0.00 °
 - Scan rate: 0.250 Hz
 - Tip velocity: 0.00 μm/s
 - Samples/line: 512
 - Lines: 64
 - Slow scan axis: Disabled
- Feedback Controls (Main):**
 - Z Modulation: Enabled
 - Tip Bias Ctl: Analog 2
 - Sample Bias Ctl: Ground
 - Aux lockin: Off
 - Integral gain: 0.7430
 - Proportional gain: 1.692
 - Amplitude setpoint: 1.828 V
 - Drive frequency: 253.593 kHz
 - Drive phase: 161.1 °
 - Drive amplitude: 607.0 mV
 - Lock-in BW: 1500 Hz
- Interleave Controls:**
 - Interleave: Enabled
 - Z Modulation: Amplitude
 - SPM feedback: Ground
 - Sample Bias Ctl: Potential
 - Input feedback: Tip
 - AC+DC Bias: Off
 - Aux lockin: 0.3716
 - Integral gain: 0.9879
 - Proportional gain: 0.2001
 - Lock-ahead gain: 0.3
 - Analog 1: 0.3
 - Analog 3: 0.3
 - Analog 4: 0.3
 - Amplitude setpoint: 1.915 V
 - Drive frequency: 253.823 kHz
 - Drive phase: 29.33 °
 - Drive amplitude: 5270 mV
 - Lock-in BW: 1200 Hz
 - Interleave mode: Lift
 - Lift start height: 0 nm
 - Lift scan height: 50.00 nm
- Channel 1:**
 - Data type: Height
 - Data scale: 75.000 nm
 - Line direction: Retrace
 - Scan line: Main
 - Realtime planefft: Line
 - Offline planefft: Full
- Channel 2:**
 - Data type: Potential
 - Data scale: 2.000 V
 - Data center: 0 V
 - Line direction: Retrace
 - Scan line: Interleave
 - Realtime planefft: None
 - Offline planefft: None
 - Highpass filter: Off
 - Lowpass filter: Off
- Other Controls:**
 - Microscope mode: Tiping
 - Z limit: 6.719 μm
 - Input gain: 0.1500
 - Input pgain: 0.3000
 - Aux input gain: 0
 - Aux input pgain: 0
 - Amplitude limit: 20.00 V
 - TM Deflection limit: 20.00 V
 - Phase limit: 360.0 °
 - X input gain: 4096
 - Y input gain: 4096
 - CX input gain: 4096
 - CY input gain: 4096
 - Units: Metric
 - Color table: 12
 - Serial number: 17900

Bottom status bar: Z: -4595.0 μm, Optics: -950.0 μm, X: 76112.7 μm, Y: 64001.6 μm, Tip#: 1.03pm 327, File: nr_gan750a 009, Capture: Off, Tip: Engaged, Surface Potential, Quadrexed D3100, NanoScope Control, NanoScope Image, Vision System.

References

- ¹ S. J. Pearton, J. C. Zolper, R. J. Shul, and F. Ren, *J. Appl. Phys.* 86, 1 (1999).
- ² H Morkoç, *Nitride Semiconductors and Devices*, Springer-Verlag Berlin Heidelberg (1999).
- ³ S Nakamura, T. Mukai, M. Senoh, *Appl. Phys. Lett.* 64, 13 (1994).
- ⁴ S. N. Mohammad, H. Morkoc, *Progress in Quantum Electronics* 20, 361-525 (1996).
- ⁵ S. Mohammad, H. Morkoc, *Proceedings of the IEEE* 83, 1306 (1995).
- ⁶ Jorg Neugebauer and Chris G. Van de Walle, *Appl. Phys. Lett.* 69, 503 (1996).
- ⁷ W. Johnson, J. Parson, M. Crew, *J. Phys. Chem.* 36, 2561 (1932).
- ⁸ H. P. Maruska and J. J. Tietjen, *Appl. Phys. Lett.* 15, 327 (1969).
- ⁹ H. Morkoc, S. Strite, G. B. Gao, M. E. Lin, B. Sverdlov, M. Burns, *J. Appl. Phys.* 76, 1363 (1994).
- ¹⁰ H. Okumura, S. Misawa, and S. Yoshida, *Appl. Phys. Lett.* 59, 1058 (1991).
- ¹¹ Amano et al., *Jpn. J. Appl. Phys.* 28 (1989).
- ¹² S. C. Jain, M. Willander, J. Narayan, R. Van Overstraeten, *J. Appl. Phys.* 87, 965 (2000).
- ¹³ Akasaki et al, *Jpn. J. Appl. Phys.* 36, 393-5408.
- ¹⁴ S. Nakamura and G. Fasol, *The Blue Laser Diodes* ~Springer, Heidelberg, (1997).
- ¹⁵ I. Vurgaftman, J. R. Meyer, and L. R. Ram-Mohan, *J. Appl. Phys.* 89, 5815 (2001).
- ¹⁶ G.P. Das, B.K. Rao, P. Jena, *Phys. Rev. B* 68, 035207 (2003).
- ¹⁷ K. Fujito, O. Mochizuki, N. Namita, Fujimura, *Phys. Status Sol.* 205, 1056 (2008).
- ¹⁸ S. Barbet et al., *Appl. Phys. Lett.* 93, 212107 (2008).
- ¹⁹ B. S. Simpkins, E. T. Yu, P. Waltereit, and J. S. Speck, *J. Appl. Phys.* 94, 1448 (2003).
- ²⁰ S.Chevtchenko, X.Ni, Q.Fan, A.A.Baski, H.Morkoç, *Appl. Phys. Lett.* 88, 122104 (2006).
- ²¹ *Phys. Rev. B.* Dahlber, Chelikowsky, Orr, 15,6, 1977.
- ²² S. Sabuktagin, M. A. Reshchikov, D.K. Johnstone, and H, Morkoc, *Mat. Res. Soc. Symp. Proc.*,798 (2004).
- ²³ V.M. Bermudez, *Appl. Phys.* 80, 15 (1996).
- ²⁴ S. Sabuktagin, M.A. Reshchikov, D.K.Johnstone, H.Morkoç, *MRS Proc* 798, Y5.39 (2004).
- ²⁵ V.M. Bermudez, *Appl. Surf. Sci.* 119 , 147 (1997).

-
- ²⁶ McAllister Technical Services, Kelvin Probe users manual, (1999-2007).
- ²⁷ G. Binnig, C.F. Quate, C. Gerber, Phys. Rev. Lett. 56, 930 - 933 (1986).
- ²⁸ Veeco, Dimension 3100 Manual, Version 4.43B (1999).
- ²⁹ Crosby, Demas, J. Phys. Chem. 75, 991-1024 (1971).
- ³⁰ M.R. Reshchikov, H. Morkoc, J. Appl. Phys. 97, 061301 (2005).
- ³¹ V. M. Bermudez, J. Appl. Phys. 80, 1190 (1996).
- ³² M.A. Reshchikov, Unpublished, "Photovoltage in GaN."
- ³³ R. A. Beach, E. C. Piquette, and T. C. McGill, MRS Internet J. Nitride Semicond. Res. 4S1, G6.26 (1999).
- ³⁴ S.M. Sze, Physics of Semiconductor Devices, 3rd ed., Wiley, New York (2007).
- ³⁵ L. Szaro, Surf. Sci. 137, 331 (1984).
- ³⁶ L. Kronik and Y. Shapira, Surf. Sci. Rep. 37, 1 (1999).
- ³⁷ S. Sabuktagin, M.A. Reshchikov, D.K. Johnstone, and H. Morkoc, Mat. Res. Soc. Symp. Proc. **798**, Y5.39 (2004)